

***On Development  
Of Ultrahard  
Hafnium and Titanium Carbide  
Materials***

---

***Emily Tholakele Maseko***



***The Degree of Magister Technologiae: Engineering Metallurgy.***

**2002**

**On Development  
Of Ultrahard  
Hafnium and Titanium Carbide  
Materials**

**BY**

**Emily Tholakele Maseko**



A Dissertation submitted to the School of Mines,  
Faculty of Engineering

Technikon Witwatersrand, Johannesburg, South Africa

In fulfillment of the requirement for the Degree of  
Magister Technologiae: Engineering Metallurgy.

September 2002

**On Development  
Of Ultrahard  
Hafnium and Titanium Carbide  
Materials**

**BY**

**Emily Tholakele Maseko**

**A Dissertation submitted to the School of Mines,  
Faculty of Engineering  
Technikon Witwatersrand, Johannesburg, South Africa  
In fulfillment of the requirement for the Degree of  
Magister Technologiae: Engineering Metallurgy.**

**Supervisor: Dr.A.F. Mulaba- Bafubiandi  
Research and Development Unit,  
Technikon Witwatersrand,  
Johannesburg, South Africa**

**Co- Supervisor: Prof.S. Luyckx  
School of Process and Materials Engineering,  
University of the Witwatersrand,  
Johannesburg, South Africa**

**September 2002**

## Declaration

I declare that this dissertation is my own work. It is being submitted for the degree of Magister Technologiae: Engineering Metallurgy at the Technikon Witwatersrand, Johannesburg. It has not been submitted before for any degree or examination in any other Technikon or University.



*E. T. Maseko* .....

E.T Maseko

..... *30<sup>th</sup>* day of *September*, year *2002* .....

## ***Dedication***

*To my parents (Moses, Elizabeth Maseko) and my grandmother (Cathrine Galagala), for their support and encouragement throughout the years. My loving husband Ronald Moratua Mokoena for having faith, encouragement and support throughout the course of this work.*



## ***Acknowledgements***

*I would like to thank my supervisors, **Dr A. Mulaba, Professor S. Luyckx** and **Dr Mathias Hermann** of the Fraunhofer Institute, Dresden, Germany for their supervision, guidance, and support and for their insistence on pursuit of excellence in all matters. **God bless you.***

*Element Six Pty (De Beer Diamond Research Laboratory) for financial support, use of their facilities and ideas.*

*Technikon of the Witwatersrand and University of the Witwatersrand for allowing me to use their facilities.*

***Most of all God almighty for everything.***

# Contents

	<b>Page</b>
<b>List of figures</b>	i
<b>List of tables</b>	iv
<b>Abstract</b>	1
<b>1. Chapter 1: Introduction</b>	2
<b>1. 2 Problem Statement</b>	4
<b>Chapter 2: Literature survey</b>	5
<b>2. Introduction</b>	6
2.1 Metals	6
2.2 The Carbides	8
2.2.1 Lattice parameter	8
2.2.2 Hardness	9
2.2.3 Hafnium Carbide	10
2.2.4 Physical properties of HfC	12
2.2.5 Mechanical properties of HfC	16
2.2.6 Chemical properties of HfC	17
2.2.7 Titanium Carbide	18
2.3 The TiC-HfC-Ni System	20
2.3.1.1 Microhardness of TiC-HfC	23
2.4 Oxidation resistance of carbides	24
2.4.1 Titanium Carbide	24
2.4.2 Hafnium Carbide	25
2.5 Synthesis of nanocrystalline TiC powders by Mechanical alloying	26



<b>3.Experimental Materials and Techniques</b>	28
<b>3.1 Introduction: Powder preparation</b>	29
3.1.1 Mixed carbides route	29
3.1.2 Single carbide route	29
3.1.3 Single Carbide Route by high-energy milling	30
3.1.3.1 Individual milling of HfC and TiC	30
3.1.3.2 High-energy milling of HfC and TiC together	31
3.1.3.3 Wet milling of HfC and TiC + Ni by High-energy mill	31
3.2 Sintering of the mixed and single carbides	32
3.2.1 Sintering mixed and single carbide without nickel	32
3.2.2 Sintering mixed and single carbide with nickel	33
3.3 Physical properties measurement	34
3.3.1 Particle size analysis	34
3.3.2 Density	34
3.3.3 Preparation of sintered specimens	36
3.4 Mechanical property measurements	37
3.4.1 Vickers hardness	37
3.4.2 Scanning electron microscopy (SEM)	37
3.4.3 XRD (x-ray diffraction)	38
<b>4. Experimental: Results and Discussion</b>	39
4. Introduction	40
4.1 Characterization of the as received powder	41
4.1.1 Powder characterization by XRD	41
4.1.2 SEM Micrographs of powders	44
4.1.3 Particle size analysis by Malvern sizer of received powders	45
4.1.4 EDS (energy dispersive spectroscopy) results from (Hf <sub>0.5</sub> Ti <sub>0.5</sub> )C <sub>0.8</sub> powder	46
4.1.5 Summary	47
4.2 Characterization of high-energy milled individual carbide powder (HfC and TiC)	48



4.2.1 Individual milled HfC powder	48
4.2.2 Individual milled TiC powder	49
4.2.3 Particle size analysis by MalvernSizer of HfC powder after high-energy milling	50
4.2.4 Particle size analysis by MalvernSizer of TiC powder after high-energy milling	51
4.2.5 d-values of individual HfC and TiC after high-energy milling	52
4.2.6 Results of grain size and strain in high-energy milled HfC and TiC (calculated by Reitveld method, IKTS)	53
4.2.7 Summary	54
4.3 Characterization of high- energy dry milled carbides mixture	55
4.3.1 XRD results of carbides mixture from high –energy milling	55
4.3.2 Examination by SEM of carbides mixture from high –energy milling	56
4.3.3 Example of EDS results of HfC + TiC+ C powder after high- energy dry milling for 12 hrs	57
4.3.4 Particle size analysis by MalvernSizer of HfC+ TiC+ C powders after high- energy dry milling	58
4.3.5 Summary	59
4.4 Characterization of sintered sample produced from pre-reacted $(\text{Hf}_{0.5}\text{Ti}_{0.5})\text{C}_{0.8}$ powder	60
4.4.1 XRD results on sintered pre-reacted $(\text{Hf}_{0.5}\text{Ti}_{0.5})\text{C}_{0.8}$ without Ni	60
4.4.2 XRD results on sintered pre-reacted $(\text{Hf}_{0.5}\text{Ti}_{0.5})\text{C}_{0.8}$ with Ni	61
4.4.3 EDS results from polished surface	62
4.4.4 SEM micrographs of $(\text{Hf}_{0.5}\text{Ti}_{0.5})\text{C}_{0.8}$ and $(\text{Hf}_{0.5}\text{Ti}_{0.5})\text{C}_{0.8} + 4\text{wt \%Ni}$ fractured surface	63
4.4.5 SEM micrographs of $(\text{Hf}_{0.5}\text{Ti}_{0.5})\text{C}_{0.8}$ and $(\text{Hf}_{0.5}\text{Ti}_{0.5})\text{C}_{0.8} + 4\text{wt \%Ni}$ polished surface	64
4.4.6 Density measurements of sintered $(\text{Hf}_{0.5}\text{Ti}_{0.5})\text{C}_{0.8}$ and $(\text{Hf}_{0.5}\text{Ti}_{0.5})\text{C}_{0.8} + \text{Ni}$	65
4.4.7 Hardness results of $(\text{Hf}_{0.5}\text{Ti}_{0.5})\text{C}_{0.8}$ and $(\text{Hf}_{0.5}\text{Ti}_{0.5})\text{C}_{0.8} + 4\text{wt \%Ni}$	65
4.4.8 Summary	66

4.5 Characterization of HfC+ TiC with 4wt% Ni produced from mixed (not milled) system	68
4.5.1 XRD results of sintered mixed (not milled) HfC+TiC+ 4wt% Ni at 1650°C	68
4.5.2 SEM micrographs of HfC+TiC+4wt% Ni sintered at 1650°C	69
4.5.3 EDS results from mixed (not milled) HfC+TiC+4wt% Ni sintered at 1650°C	70
4.5.4 Hardness results	70
4.5.5 Discussion	71
4.6 Characterization of material produced from high- energy dry milled HfC+TiC+C powder with and without 4wt% Ni	72
4.6.1 XRD results from HfC+TiC +C sintered without 4wt %Ni at 2000°C	72
4.6.2 XRD results from HfC+TiC+C sintered with 4wt %Ni at 1650°C	73
4.6.3 SEM micrographs of high-energy milled HfC+TiC+C with and without Ni	74
4.6.4 SEM micrographs of high-energy milled HfC+TiC+ C with and without Ni	75
4.6.5 Example of EDS from high-energy dry milled HfC+TiC+C with and without 4wt %Ni	76
4.6.6 Vickers hardness results from high-energy dry milled HfC+TiC+C with and without Ni	77
4.6.7 Results of density of high-energy dry milled HfC+TiC+C with and without Ni	78
4.6.8 Discussion	
<b>5. Final Discussion and Conclusion</b>	<b>79</b>
<b>6. References</b>	<b>80</b>
Appendix 1	82
Appendix 2	83
Appendix 3	84
Appendix 4	85
Appendix 5	86

Appendix 6	87
Appendix 7	88
Appendix 8	89
Appendix 9	90
Appendix 10	91
Appendix 11	92



## List of Figures

	Page
<b>Chapter 2: Literature study</b>	
2.1 Body centered cubic structure	6
2.2 Hexagonal closed packed structure	7
2.3 Schematic calculated phase diagram for Zr, Ti, Hf	7
2.4 Lattice parameter as a function of carbon content	8
2.5 hardness of TiC and HfC as a function Carbon content	9
2.6 Binary phase diagram indicating HfC transition	11
2.7 Dilatometer measurements of thermal expansion	12
2.8 X-ray diffraction measurements of HfC	13
2.9 The lattice parameter of HfC as a function of stoichiometry according to dates given by authors cited	15
2.10 Yield stress of group iv carbides as a function of temperature	16
2.11 The composition of HfC as a fuction of nitrogen pressure	17
2.12 Binary phase diagram of TiC	18
2.13 TiC-HfC phase diagram	21
2.14 Ti-Hf-Cat 800°C, single phase, two phase, three phases alloy	22
2.15 Temperature dependence of microhardness of group iv –vi carbide	23
2.16 X-ray patterns of Ti/C (mol) = 1:1 at different milling time	26
2.17 The relation between nanocrystalline size and milling	27
<b>Chapter 3: Experimental work</b>	
3.1 Schematic diagram of micronizer mill	29
3.2 High energy mill PM400/2	30
3.3 Schematic of graphite pot in which the powder is placed for sintering	32
3.4 Diagram showing sintering cycle for single and mixed carbide without Ni	33
3.5 Diagram showing sintering cycle for single and mixed carbide with Ni	34

## Chapter 4: Experimental results and Discussion

4.1 XRD results of $(\text{Hf}_{0.5}\text{Ti}_{0.5})\text{C}_{0.8}$ powder from Japan New Metals	41
4.2 XRD results of HfC powder from Japan New Metals	42
4.3 XRD results of TiC powder Good fellows Metals	43
4.4 SEM micrographs of the powders as received from suppliers	44
4.5 Particle size analysis of HfC powder as received	45
4.6 Particle size analysis of TiC powder as received	45
4.7 Particle size analysis of $(\text{Hf}_{0.5}\text{Ti}_{0.5})\text{C}_{0.8}$ received powder	46
4.8 EDS spectra of $(\text{Hf}_{0.5}\text{Ti}_{0.5})\text{C}_{0.8}$ powder	46
4.9 XRD results of HfC powder individual mill from Japan New Metals	48
4.10 XRD results of TiC powder individual mill	48
4.11 Particle size analysis showing change in particle size of HfC powder after high- energy milling	49
4.12 Particle size analysis showing change in particle size of TiC powder after high- energy milling	50
4.13 Particle size analysis showing change in particle size of TiC powder after high- energy milling for 2hrs	51
4.14 Particle size analysis showing change in particle size of TiC powder after high- energy milling for 6hrs	51
4.15 XRD results of HfC+TiC+ carbon black powder after high- dry energy milling for 12 hrs	55
4.16 SEM micrographs of the $(\text{Hf}_{0.5}\text{Ti}_{0.5})\text{C}_{0.8}$ and high-energy dry milled HfC +TiC+ carbon black	56
4.17 EDS spectra of HfC +TiC after high- energy dry milled for 12 hrs	57
4.18 Particle size analysis showing change in particle size of HfC +TiC + carbon black powder after high- energy milling for 12 hours	58
4.19 XRD results of $(\text{Hf}_{0.5}\text{Ti}_{0.5})\text{C}_{0.8}$ sintered at 2000°C	60
4.20 XRD results of $(\text{Hf}_{0.5}\text{Ti}_{0.5})\text{C}_{0.8}$ + 4% Ni sintered at 1650°C	61

4.21 EDS spectra on $(\text{Hf}_{0.5}\text{Ti}_{0.5})\text{C}_{0.8}$ , $(\text{Hf}_{0.5}\text{Ti}_{0.5})\text{C}_{0.8}$ + 4% Ni fractured and polished surface	62
4.22 SEM Micrographs of $(\text{Hf}_{0.5}\text{Ti}_{0.5})\text{C}_{0.8}$ and of $(\text{Hf}_{0.5}\text{Ti}_{0.5})\text{C}_{0.8}$ + Ni fracture surface	63
4.23 SEM Micrographs of $(\text{Hf}_{0.5}\text{Ti}_{0.5})\text{C}_{0.8}$ and of $(\text{Hf}_{0.5}\text{Ti}_{0.5})\text{C}_{0.8}$ + Ni polished surface	64
4.24 XRD results of HfC+TiC+ 4wt% Ni sintered at 1650°C	66
4.25 SEM micrographs of HfC+TiC+ 4wt% Ni sintered at 1650°C of fractured and polished surface	69
4.26 EDS spectra of HfC+TiC+ 4wt% Ni sintered at 1650°C of fractured and polished surface	70
4.27 XRD results of HfC + TiC sintered without Ni at 2000°C	72
4.28 XRD results of HfC + TiC sintered with 4wt% Ni at 1650°C	73
4.29 SEM Micrographs of High- energy dry milled with and without Ni fracture surface	74
4.30 SEM Micrographs of High- energy dry milled HfC+TiC with and without Ni polished surface	75
4.31 EDS spectra of High- energy dry milled HfC+TiC with and without 4% Ni fracture and polished surface	76

## List of table

	<b>Page</b>
<b>Chapter 2</b>	
2.1 Physical properties of HfC	14
<b>Chapter 3</b>	
3.1 Parameters used in high-energy mill	31
3.2 Parameters used in particle size analysis	35
3.3 Parameters which were used for analysis in XRD	36
<b>Chapter 4</b>	
4.1 HfC d-values vs milling time	52
4.2 TiC d-values vs milling time	52
4.3 Results of grain size and strain in HfC and TiC (Rietveld Method: IKTS)	53
4.4 Density measurements of $(\text{Hf}_{0.5}\text{Ti}_{0.5})\text{C}_{0.8}$ and of $(\text{Hf}_{0.5}\text{Ti}_{0.5})\text{C}_{0.8} + 4\text{wt}\% \text{Ni}$	65
4.5 Vickers hardness of $(\text{Hf}_{0.5}\text{Ti}_{0.5})\text{C}_{0.8}$ and of $(\text{Hf}_{0.5}\text{Ti}_{0.5})\text{C}_{0.8} + 4\text{wt}\% \text{Ni}$	65
4.6 Vickers hardness for mixed carbides HfC+ TiC+ C+4wt% Ni	70
4.7 Vickers hardness high-energy dry milled HfC+ TiC+ C	77
4.8 Density measurements of high-energy dry milled HfC+ TiC+ C	77

## Abstract

A mixture of HfC and TiC powders and a (Hf,Ti)C powder have been hot pressed with 4wt% Ni. In the absence of Ni the hot pressed temperature was 2000°C and in the presence of Ni 1650°C. The pressure of 30 MPa was applied in both cases.

The starting powders were substoichiometric, as deduced from XRD spectra analyses, and the (Hf,Ti)C powders consisted of a range of compositions, as indicated by the width of the XRD peaks.

In the absence of Ni the powders sintered without the formation of a liquid phase. In the case of HfC and TiC mixture, high- energy dry milled HfC + TiC +C black powder sintering occurred with simultaneous formation of (Hf,Ti)C solid solution. On account of mutual solid solubility of two carbides vacancy interdiffusion controlled the solution as well as the sintering process, assisted by the high concentration of vacancies in the starting powders. In the case of (Hf,Ti)C powder diffusion was also the controlling process because the solid solution was not homogeneous and the system tended to homogenization, as shown by the narrowing of the XRD peaks after sintering. Since the diffusion of HfC into TiC did not occur at the same rate as the diffusion of TiC into HfC (as expected, on account of the different melting points of the two materials) diffusional porosity was observed in some of the (Hf, Ti) C grains. Grain growth was substantial but uniform.

In the presence of Ni, sintering occurred with the formation of a liquid phase. The volume fraction of the liquid phase formed was sufficient to yield a low porosity. Grain growth was less than in the case of material sintered without Ni, probably just on account of lower sintering temperature.

In the case of high- energy dry milled the reduction in particle size was observed.



# Chapter 1

## INTRODUCTION

## 1. Introduction

Refractory (Ti,Hf)C are important ceramic because of their high hardness, high melting point and strength at elevated temperatures. According to the literature a solid solution of (Hf,Ti)C can reach very high microhardness, depending on the molar ratio of HfC to TiC and the carbon content. It has been reported that at a molar ratio of  $\frac{\text{Hf}}{\text{Ti}} \cong \frac{60}{40}$  values of microhardness of 4600 HV can be reached (Paderno, 1967). The hardness of solid the solution (Hf,Ti)C must also depend on the carbon content since this is true for both carbides HfC and TiC, with the highest hardness value obtained close to stoichiometric carbon content (Ramqvist, 1969). Although (Hf, Ti) C is technologically interesting on the account of its high potential hardness, very few investigations on this material are found in literature, which may be due to the high cost of (Hf,Ti)C powders (Perry, 1987).

The aim of this investigation was to produce a (Hf, Ti) C sintered material of high hardness using different routes: -

- (i) From pre-reacted (Hf, Ti) C powder
- (ii) From HfC +TiC+ Ni powder mixed by micronizing mill
- (iii) From high-energy dry milled HfC +TiC+ C powder

The powders were sintered with and without binder. The binder selected was Ni because the wettability of both HfC and TiC by Ni is higher than by the other metals (Co and Fe), which are typically used as binders for carbides (Ramqvist, 1965). The amount of binder was kept to a minimum (4wt %) since the ultimate aim was to produce materials of high hardness.

This work is divided into the following chapters: -

1. Introduction
2. Literature Survey
3. Experimental
4. Results and discussion
5. Conclusion

The literature survey in chapter 2 summarizes the available knowledge on HfC, TiC and on the Hf-Ti-C system.

Chapter 3 details the powders processing and sintering routes. It also details the properties measured after sintering and how they were measured.

The results and discussion in chapter 4 detail the characterization of powders as received and after high- energy milling and the characterization of the sintered materials.

Chapter 5 summarizes the conclusion that can be drawn from the results obtained.

### **1.1 Problem Statement**

Can a (Hf, Ti) carbide, be synthesized using ultra hard conventional route and mechanical alloying?

# **Chapter 2**

## **LITERATURE SURVEY**

## 2. Introduction

This chapter summarizes the available knowledge on the Ti-Hf-C system, which is relevant to this work, starting from Ti and Hf metals.

### 2.1 The metals

Titanium and hafnium crystallize in a slightly compressed hcp type structure and transform to bcc (shown in figure 2.1 and 2.2) at high temperature as shown in figure 2.3. Titanium remains in the hcp structure up to at least 87 GPa. These transition metals in form of carbides have extreme hardness and high melting point. HfC and TiC form a solid solution (Cahn, 1996).

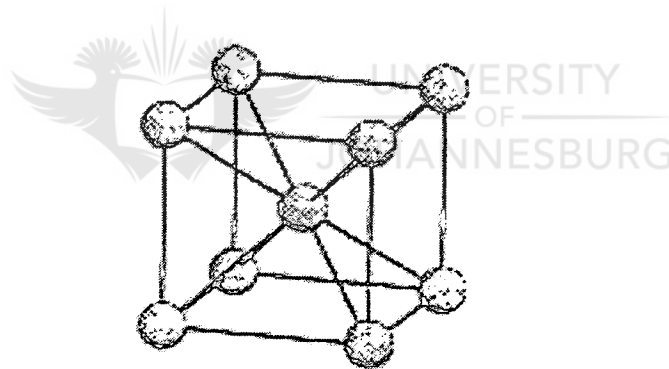


Figure 2.1: Body centered cubic structure (Cahn, 1996)

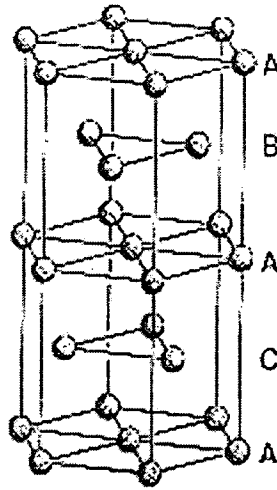


Figure 2.2: Hexagonal closed packed structure (Cahn, 1996)

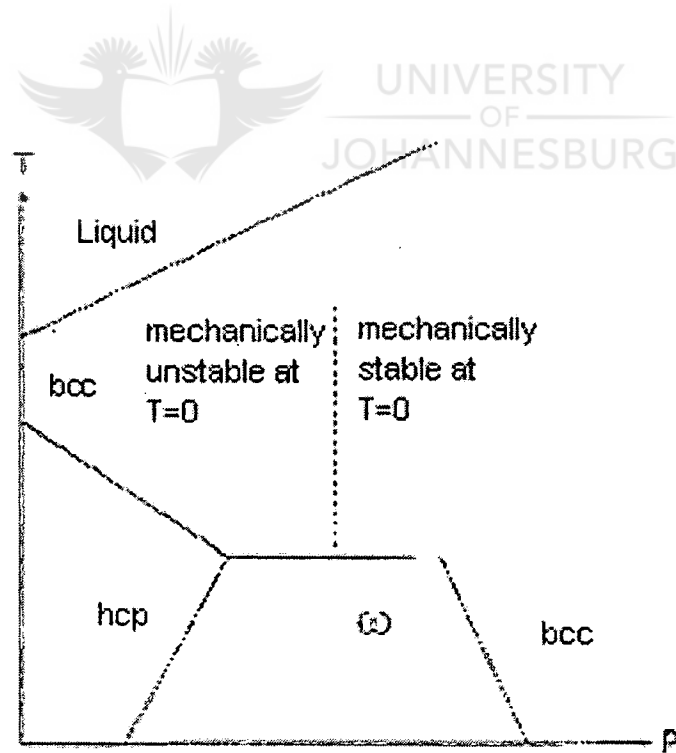


Figure 2.3: Schematic calculated phase diagram for Ti and Hf ( $\omega$ - omega phase) (Cahn, 1996).

## 2.2 The Carbides

Refractory carbides (transition-metal carbide of group ivb TiC, ZrC, HfC) have been successfully used in the metal industry due to their high hardness, high melting points and strength at elevated temperatures.

### 2.2.1 Lattice parameters

Measurements of the x-ray diffraction patterns of the carbides are very important to identify phases, determine lattice parameters and homogeneity of carbides. Parameters measured can be used advantageously as an indirect analysis method for carbon and dissolved oxygen and nitrogen. Oxygen and nitrogen decrease the lattice parameter of group ivb Ti, Hf carbides. The variation of lattice parameter with carbon content of TiC and HfC is show in figure 2.4 (Ramqvist, 1969).

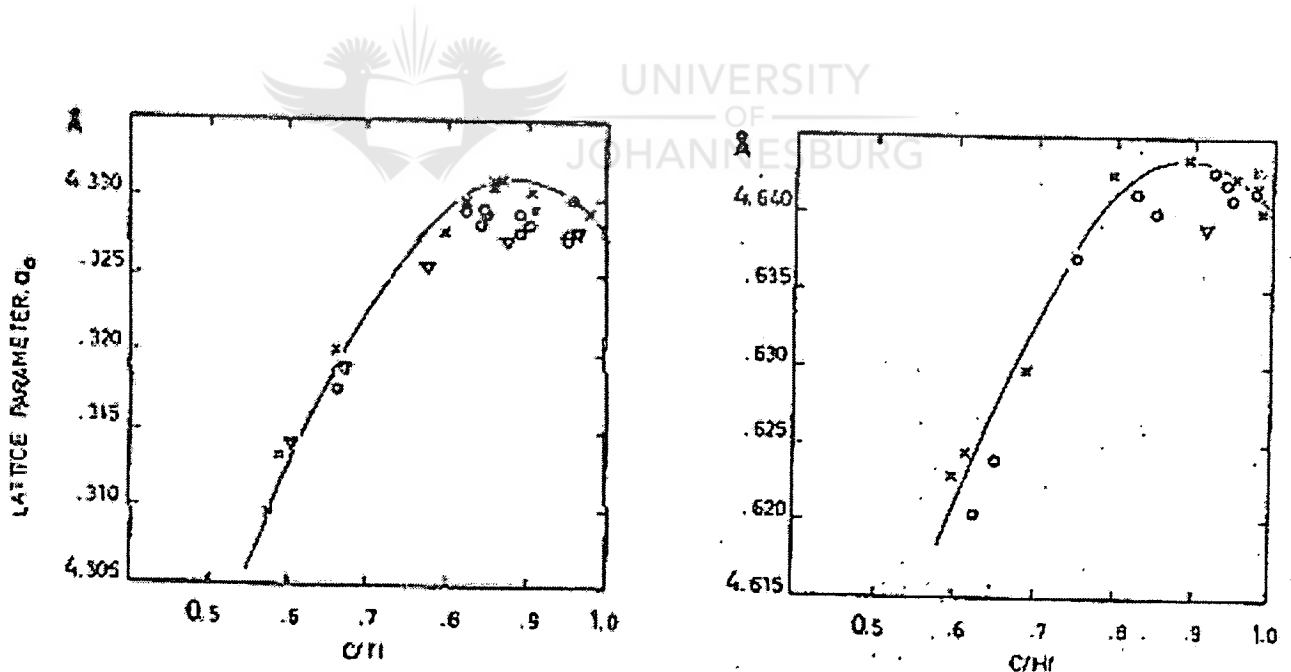


Figure 2.4: Lattice parameter as a function of carbon content of TiC and HfC

(Ramqvist, 1969)

### 2.2.2 Hardness

The hardness of TiC and HfC increases with the increase in carbon content as shown in figure 2.5 (Ramqvist, 1969). The hardness of TiC and HfC was shown to be heavily affected by dissolved gases, together with the influence of carbon content.

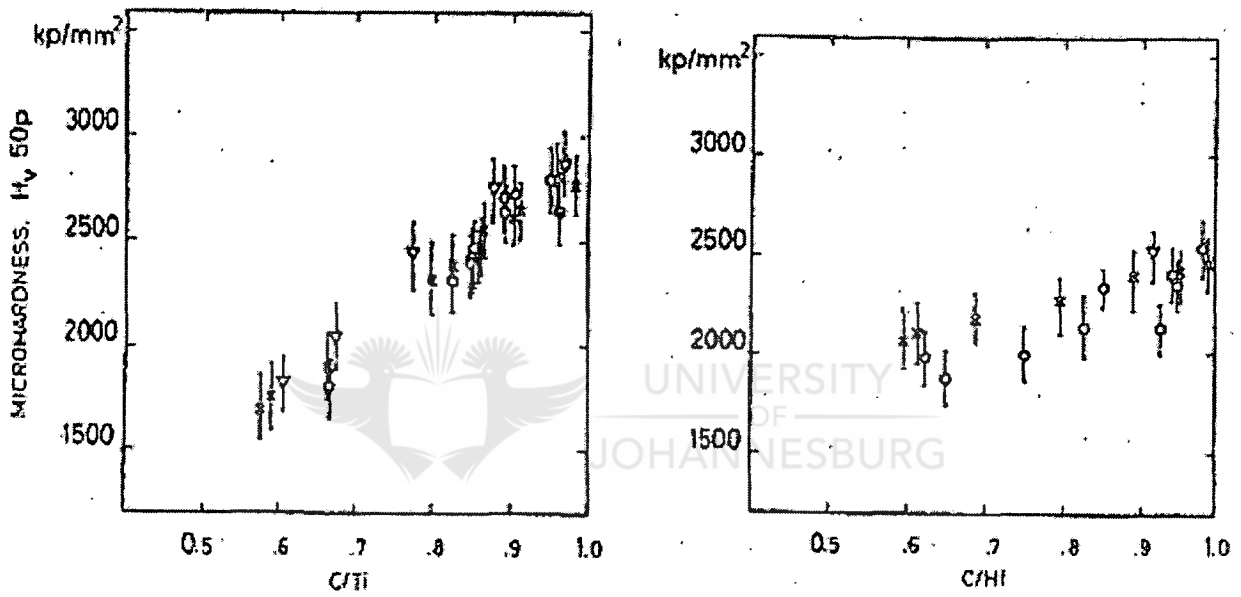


Figure 2.5: Hardness of TiC and HfC as a function of carbon content (Ramqvist, 1969).



### 2.2.3 Hafnium Carbide

The purest HfC can be produced by reacting the elemental powders either by arc melting or by powder metallurgy (Edmund, 1967). Like other elements in the group, Hf does not react quickly with carbon. HfC is very difficult to obtain in an oxygen-free state. Other researcher's experimental work showed that HfC is most difficult to purify, of all carbides.

Only by melting or heating in good vacuum above  $\sim 2500^{\circ}\text{C}$  can the oxygen content be reduced to acceptable level. Grey coloured hafnium carbide (6.30 w/o carbon) is only intermediate phase found in the hafnium carbon system. It exists over a wide range below and up to the stoichiometric composition (Edmund, 1967).

The binary phase diagram of the HfC system is shown in figure 2.6. A compound of Hf-C system is formed in the homogeneity range of 34 to 38 %C at  $2200^{\circ}\text{C}$  and 36 to 49.3 at %C at  $3150^{\circ}\text{C}$ , with a content of 47.5 at %C. HfC melts at  $3830^{\circ}\text{C}$ . The eutectic Hf-C system is formed at  $3150^{\circ}\text{C}$  and the composition at eutectic point corresponds to 66 at %C (Upadhyaya, 1996).

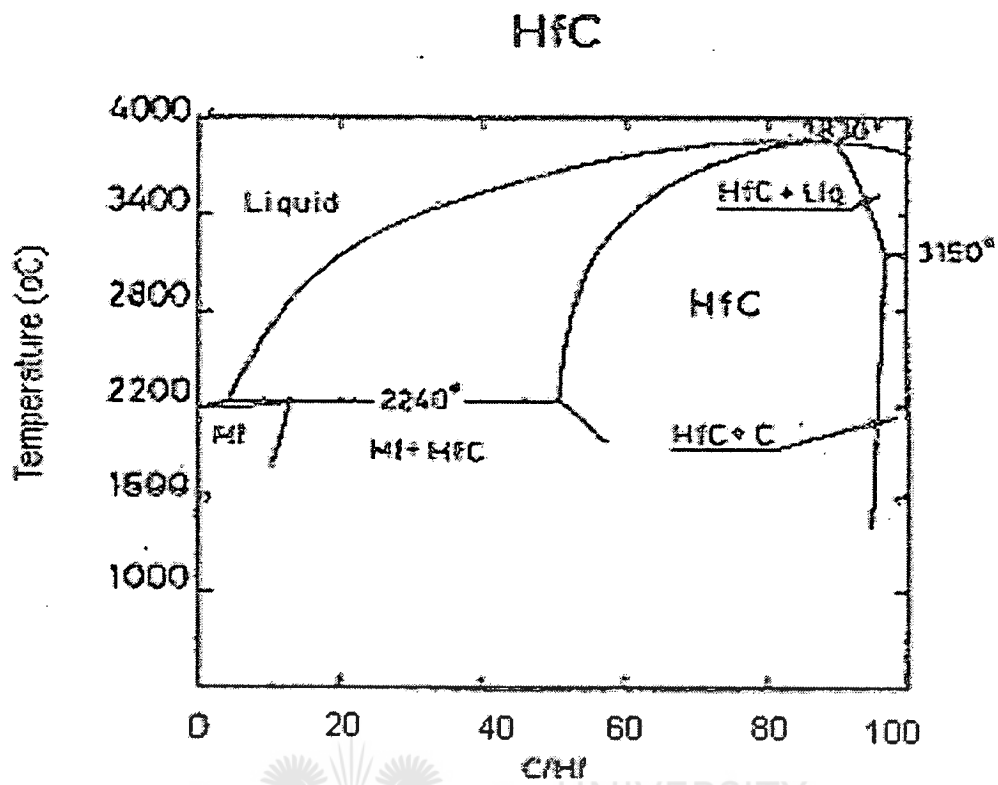


Figure 2.6: Binary phase diagram indicating HfC transition from Hf and C (Okamoto, 1990)

### 2.2.3.1 Physical Properties

The electrical resistivity, thermal expansion and density of HfC have been measured. There appear to be a systematic difference (Adams, 1968) in the values of thermal expansion depending upon whether they were measured by dilatometry, which gives higher values, or by lattice parameter determination. Curves for both are given in figure 2.7 and 2.8 respectively.

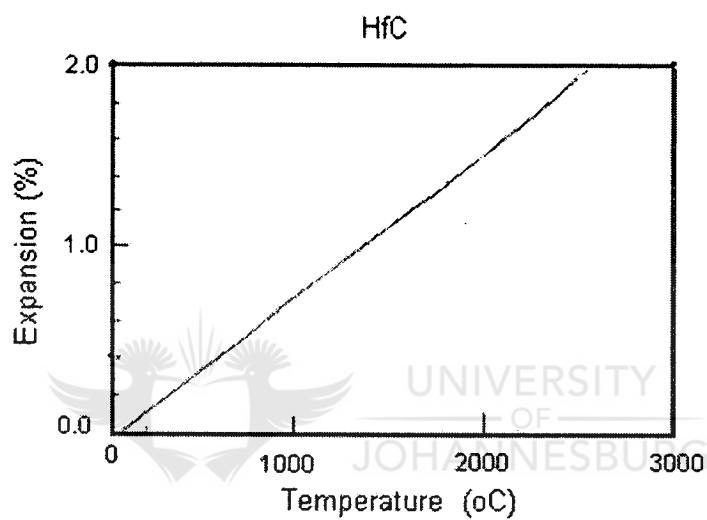
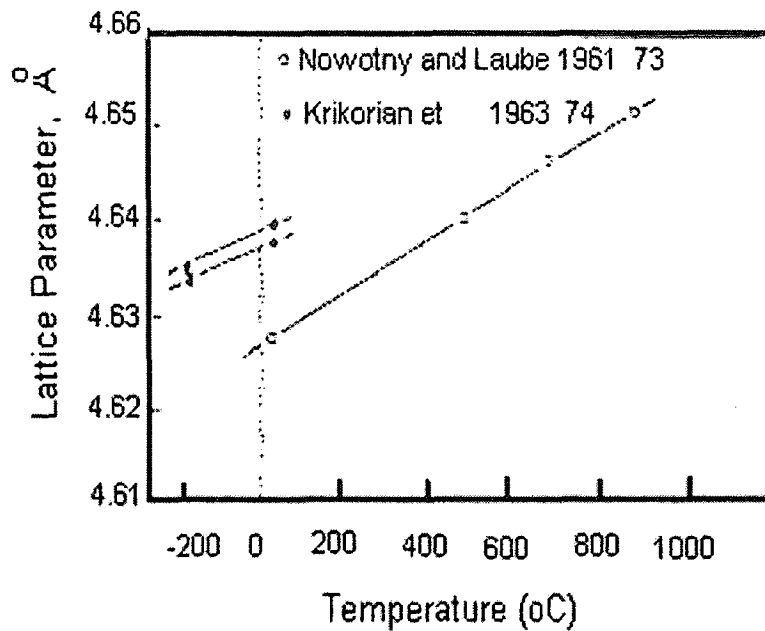


Figure 2.7: Dilatometer measurement of the thermal expansion of HfC  
(Perry, 1987)



**Figure 2.8:** X-ray diffraction measurements of the lattice parameter of HfC at various temperatures (Perry, 1987).

The lattice parameter has been measured at low and elevated temperatures as show in figure 2.8 to allow thermal expansion to be derived ( table 2.1). The difference in the lattice parameters at ambient temperature in figure 2.8 should be taken in the context of the wide band of values reported at stoichiometric compositions as shown in figure 2.9.

**Table 2.1:** Physical properties of HfC (Perry, 1987)

Authors	year	resistivity $\mu\Omega$ cm	Thermal expansion $\times 10^{-6}$ K <sup>-1</sup>	Density g/cm <sup>3</sup>
Moers	1931	109		
Becker	1933			12.2
Cotter and Kohn				
	1954			12.4...12.6
Nowotny et al.	1959			12.3
Grisaffer	1960		6.59 (25...612 °C) <sup>d</sup>	
Krikorian	1960		6.32 (25...500 °C) <sup>d</sup>	
			6.26 (25...1000 °C) <sup>d</sup>	
Krikorian	1963		4.1± 0.7 (-190 to + 26°C) <sup>x1</sup>	
			4.3± 0.4 (-190 to + 26°C) <sup>x2</sup>	
			3.5± 0.4 (-190 to + 26°C) <sup>x3</sup>	
Brizes	1970		6.725 (100 °C) <sup>d</sup>	
			7.353 (1000 °C) <sup>d</sup>	
			6.725 (2000 °C) <sup>d</sup>	

d= dilatometer, x= lattice parameter, 1= HfC<sub>0.89</sub> 2= HfC<sub>0.97</sub> 3= HfC<sub>0.95</sub>

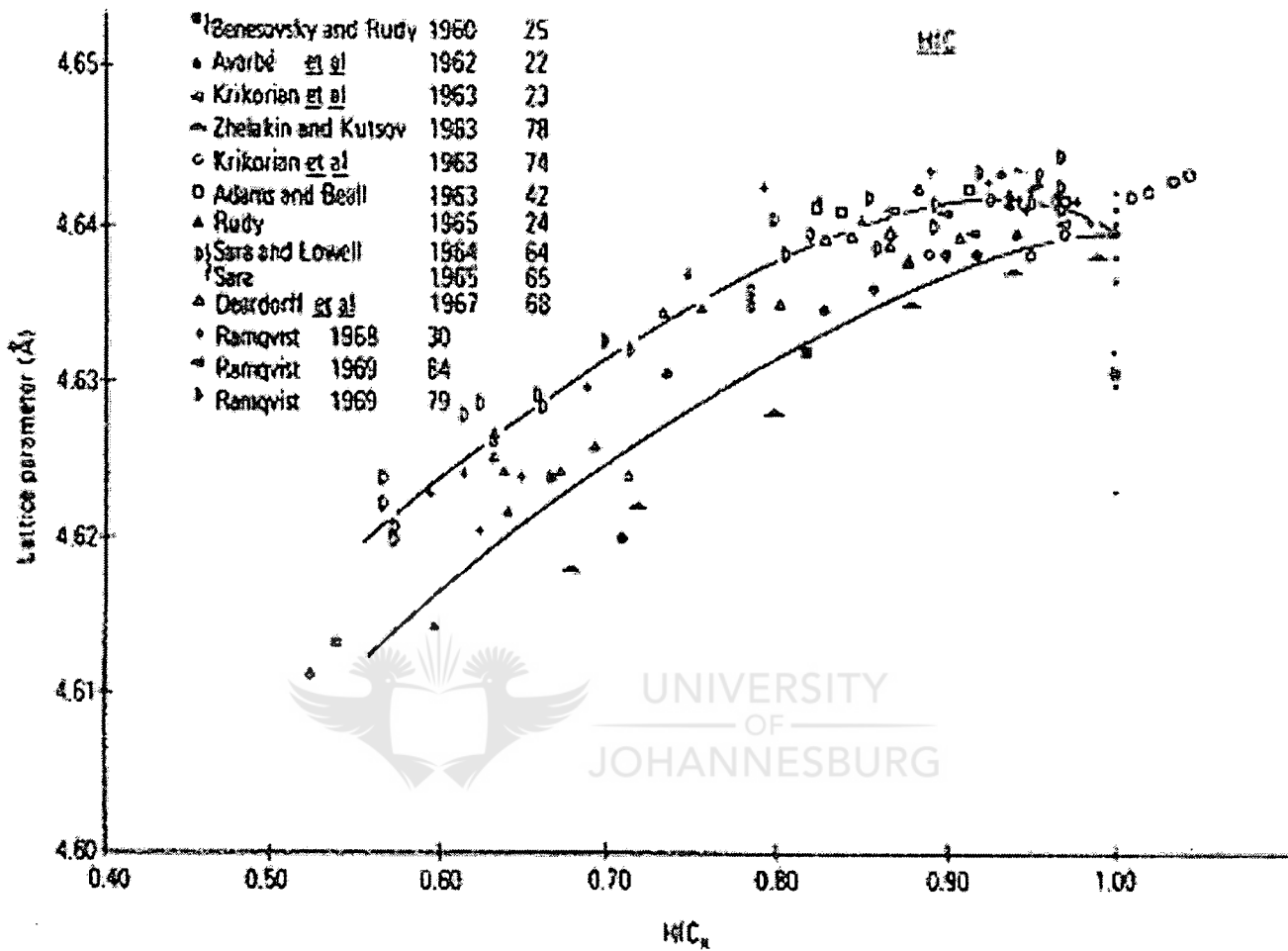


Figure 2.9: The lattice parameter of Hf-C system as a function of stoichiometry (Perry, 1987)

### 2.2.3.2 Mechanical properties

The deformation of a large high purity, fully dense HfC sample was studied as a function of temperature by Brizes (1970). He studied the yield stress and found it to be thermally activated up to 0.7 of the melting point. In comparison with properties of the other group IV carbides, the yield stress is lower for higher atomic number carbides at low temperature but the situation reverses at elevated temperatures as shown in figure 2.10 also found that the constant load creep rate is lower than that of the other group IV carbides.

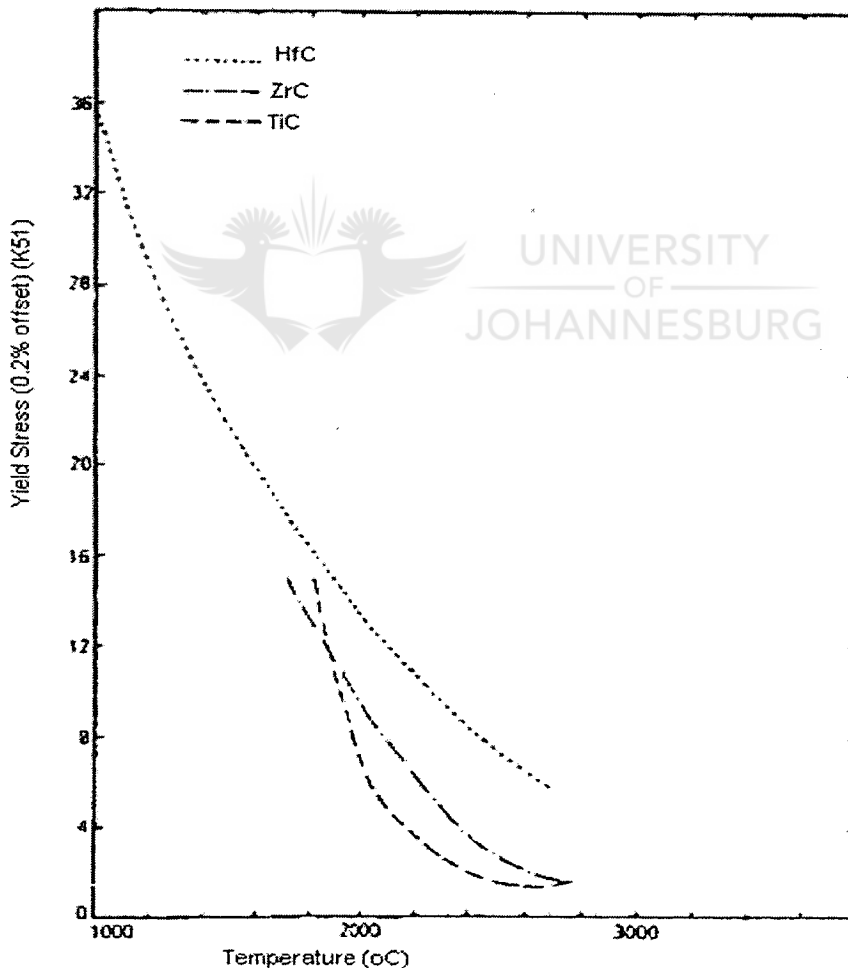


Figure 2.10: Yield stress of group IV carbides as a function of temperature (Perry, 1987)

### 2.2.3.3 Chemical Properties

Kieffer et al (1971) at 1400°C and at pressures of 1,30 and 300 atmosphere, found that HfC absorbed nitrogen quite readily even at one atmosphere pressure. At higher pressure as much as 50% of the carbon could be replaced by nitrogen figure 2.11. This carbon is released as graphite in practical terms, adversely affects the sintering of such materials (Perry, 1987).

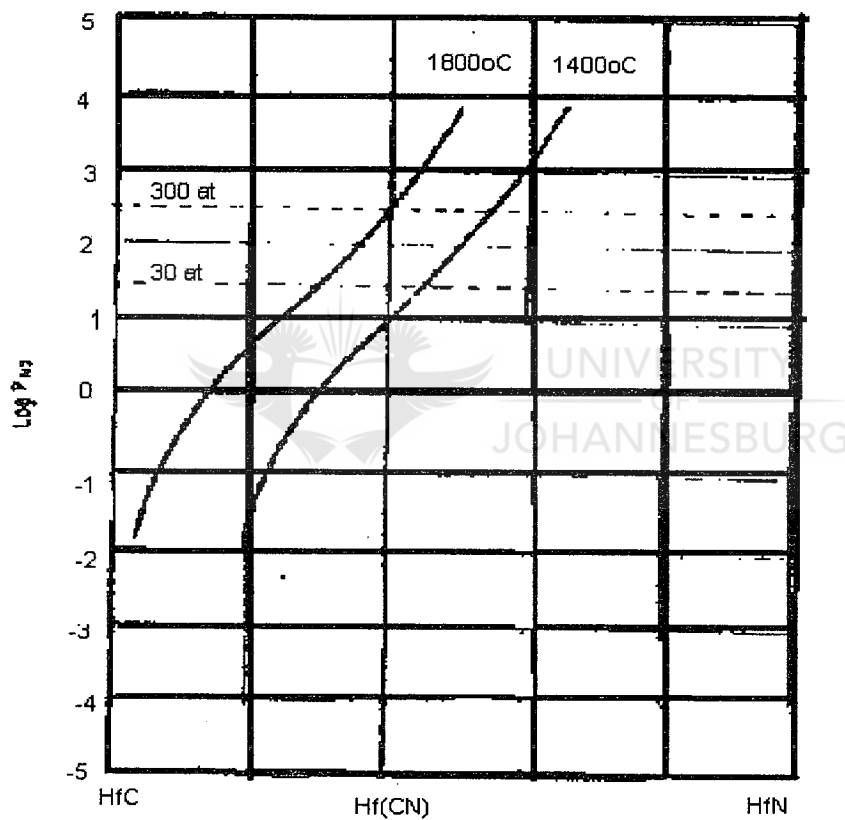


Figure 2.11: The composition of HfC as a function of nitrogen pressure (Perry, 1987)



## 2.2.4 Titanium carbide

Titanium carbide exists as a compound which is a single phase over a range from 35 to somewhat less than 50 atomic % C. The compound with the highest melting point has a composition somewhat below that of stoichiometric TiC. The carbon and oxygen content of the carbide affect the cutting properties of cemented carbides containing TiC (Murray, 1987).

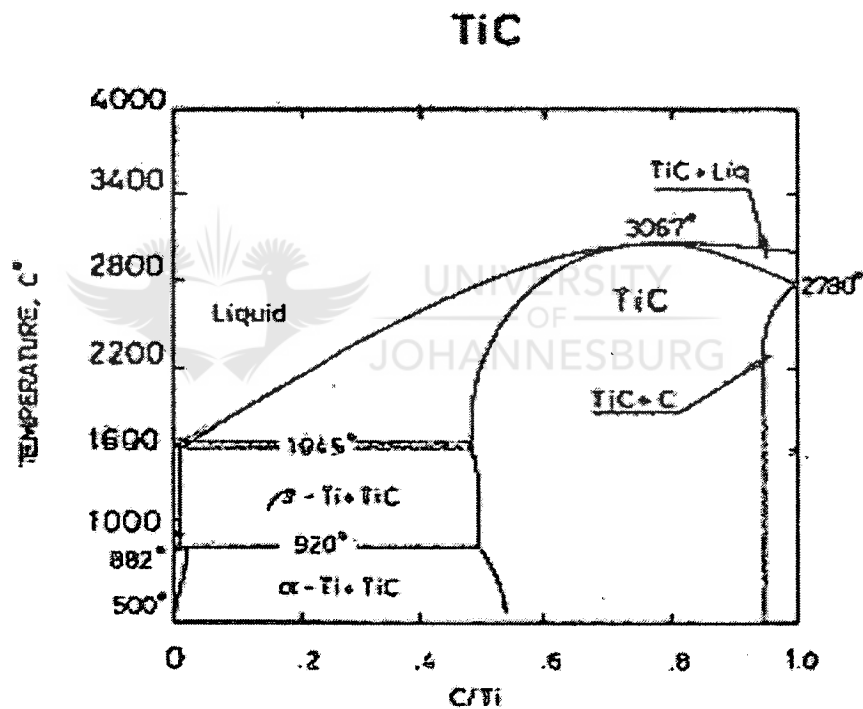


Figure 2.12: Binary phase diagram of TiC (Murray, 1987)

Titanium carbide  $TiC_\gamma$  has the widest region of homogeneity among carbides of group IV (from  $TiC_{0.48}$  to  $TiC_{1.00}$ ). The presence of nonstoichiometry may under certain conditions lead to redistribution of carbon atoms and structural vacancies, as well as to formation of various ordered cubic phases, which have a lattice spacing twice as large as that of disordered carbide.

Measurements of the microhardness  $H_v$  of  $TiC$  before and after annealing have shown that as the carbon of  $TiC_\gamma$  is raised from  $y=0.6$  to  $y=0.9$ , the microhardness increases by a small amount, while on going to a stoichiometric composition carbide  $TiC_{1.0}$ , there is a dramatic increase in microhardness. In the  $TiC$  system in figure 2.12 it has been found that there is a short range order in  $TiC$  from  $C/Ti \sim 0.5$  to  $\sim 0.64$  and long range order in carbon atoms at temperature below  $900^\circ C$ . There is a variation in the lattice parameter as a function of  $TiC$  composition in the homogeneity range (Upadhyaya, 1996).

## 2.3 The TiC-HfC-Ni system

The TiC-HfC-Ni system was studied by Mun and Kang (1999) by infiltrating Ni. A phase separation of (Ti, Hf) C and (Hf, Ti) C was noted when > 20 wt-% HfC was added to TiC-HfC-Ni. In the TiC-HfC-Ni, the high surface energy of the TiC phase in liquid Ni caused a rapid coalescence of TiC particles if the carbide content was smaller than 5 wt%. As the HfC increases to more than 10wt% the system showed a poor sinterability with numerous entrapped pores (Mun, 1999). The (Ti, Hf) C solid solution was the major phase observed in the microstructure, owing to undissolved HfC where a (Ti, Hf) C solid solution precipitated. The initial particle size of HfC was about 10  $\mu\text{m}$ , it is possible for the HfC phase to have remained as undissolved material owing to the limited sintering time.

The phase separation of HfC and TiC would be expected to take place in the (Ti, Hf) C solid solution below 1700°C as shown by phase diagram in figure 2.13. The miscibility gap is located in the range 8-68 wt% HfC at 1400°C. In the case of TiC- 20HfC-20Ni where the ratio of HfC/ (TiC+HfC) is 0.25, the microstructure appears homogeneous and no phase separation is evident. The discrepancy in the range for the separation can be attributed to the non-equilibrium state of the phases caused by rapid cooling and, possibly, to the presence of liquid Ni (Mun, 1999).

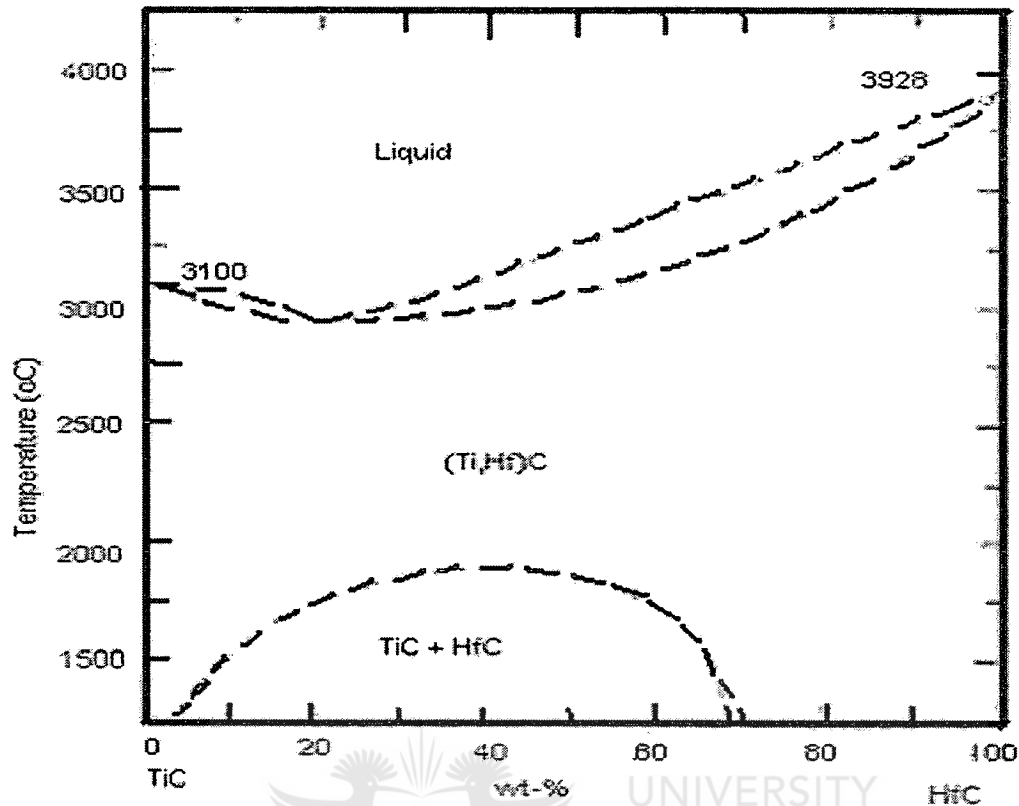
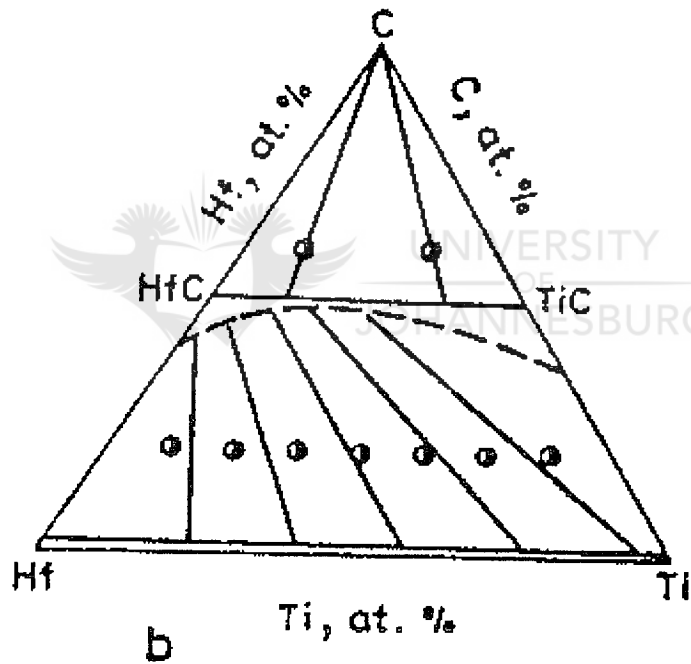


Figure 2.13: TiC-HfC phase diagram (Mun, 1999).

The wettability of liquid Ni on HfC is known to be poor compared with that of TiC, the surface energy between HfC and liquid Ni is higher than that between TiC and liquid Ni. TiC has a greater tendency to dissolve in the Ni binder than HfC. The growth rate (Hf,Ti)C increases with HfC content, sintering for 24hrs the particle size became larger about 10-20  $\mu\text{m}$  (Mun, 1999).

The Ternary (Ti, Hf)C system is similar to the (Ti, Zr)C system (Voroshilov, 1967). However in the system Ti–Hf- C at 800 °C the discontinuity of solubility is not observed (figure 2.14). Jangg, Kieffer and Usner, (1968) did not succeed in producing solid solutions in the system TiC-HfC. Existence of two phase areas in the TiC-HfC the system in the temperature interval 1200 to 1900 °C (figure 2.13) was illustrated by Kieffer et al.



**Figure 2.14:** Ti-Hf-C at 800 °C; two phases alloys (Kieffer, 1968)

### 2.3.1 Microhardness of TiC-HfC

The microhardness of the solid-solution of the systems TiC-HfC, ZrC-HfC, TaC-HfC, etc was studied by Paderno, 1967. It was found that all systems have a maximum in the curve of the microhardness as a function of composition. Kovalchenko and others (1991) studied the temperature dependence of the hardness of Ti, Zr, and Hf monocarbides. At low temperature the activation energy for TiC, ZrC, HfC is 0, 63; 0, 43 and 0, 74 eV. In the high temperatures range (over 1670K), the activation energy for plastic flow of Ti and Zr carbides increases to 2, 38 and 2, 58 eV. Figure 2.15 shows the temperature dependence of hardness for selected refractory carbides.

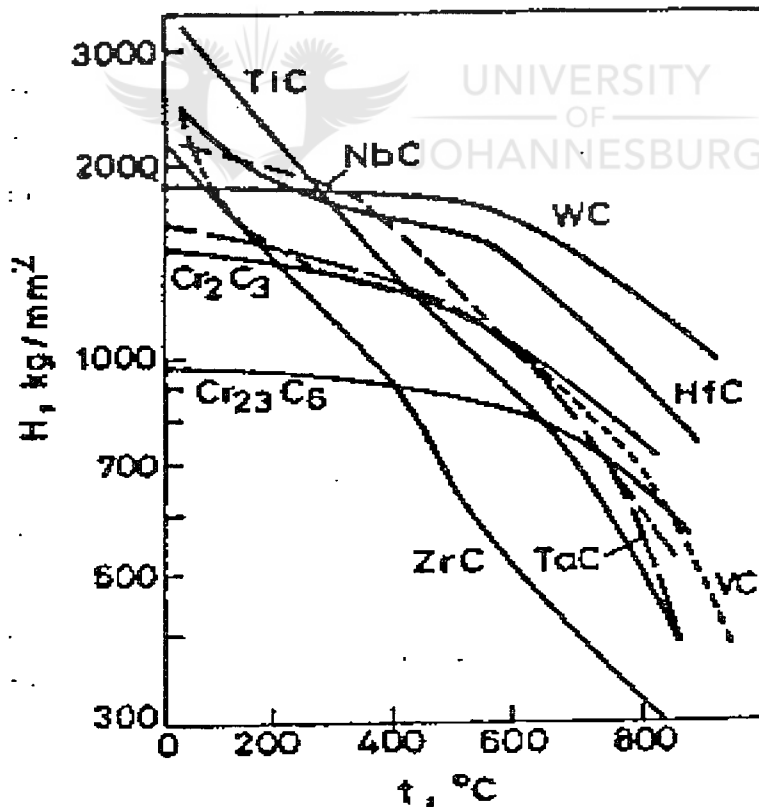


Figure 2.15: Temperature dependence of microhardness of group iv-vi metal carbide (Westbrook, 1962)

## 2.4 Oxidation resistance of the carbides

Refractory carbides find extensive applications under conditions of low vacuum and low oxygen pressure and high temperature. Their oxidation behavior is given below:

### 2.4.1 Titanium Carbide

Oxidation investigation on titanium carbide (TiC) sintered compacts was carried out in the range of 400 to 1000°C by Samsonov and Golubeva (1956). Chemical, and x-ray diffraction studies of oxide films showed that in the first stage of oxidation a dense film of solid solution TiC-TiO is formed as a result of introducing of oxygen atoms at sites not occupied by carbon, then, oxygen diffuses through the solid solution layer to form the higher oxides Ti<sub>2</sub>O<sub>3</sub> and TiO<sub>2</sub>.

The apparent activation energy for diffusion of oxygen ions through the solid solution layer, was found to be 179,7 kJ/mole (429000 kcal/ mole). Investigations into the atmospheric oxidation of TiC at temperatures of 500 to 1500 °C have established that the process is accompanied by solution of oxygen in its lattice and the formation of a oxycarbide solid solution.

## 2.4.2 Hafnium Carbide

Berkowitz, (1967) did oxidation studies of HfC produced by zone melting in oxygen under a pressure of about 10 atm over the temperature range 1790 to 2000 K. It was found that under these conditions oxidation could be expressed as a linear function, and took place mainly at the grain boundaries.

Voitovich and Pugach, (1973) studied oxidation of HfC in air in the temperature range 500 to 1200°C for 5 hours exposure. Results showed that up to 700°C, HfC showed virtually no oxidation, but already at 800°C the scales formed on it began to detach themselves from the specimens. X-ray analysis showed that the monoclinic HfO<sub>2</sub> phase normally formed during oxidation of metallic hafnium is the not only oxide present in the scales produced during the oxidation of HfC, as it is joined there by the tetragonal HfO<sub>2</sub> phase. The mechanism controlling oxidation was found to be the reaction at the scale/ carbide interface.



## 2.5 Synthesis of nanocrystalline TiC powder by mechanical alloying

This work was done by Xinkun and associates (2001). The raw powders of Ti and C were both less than 200 mesh, greater than 99% wt in purity. These powders were mixed by a mole ratio of 1:1 and milled in GN-2 ball milling. The powders were analysed by XRD, EPMA and TEM. The results figure 2.16 shows that TiC can be synthesized in a short time at room temperature.

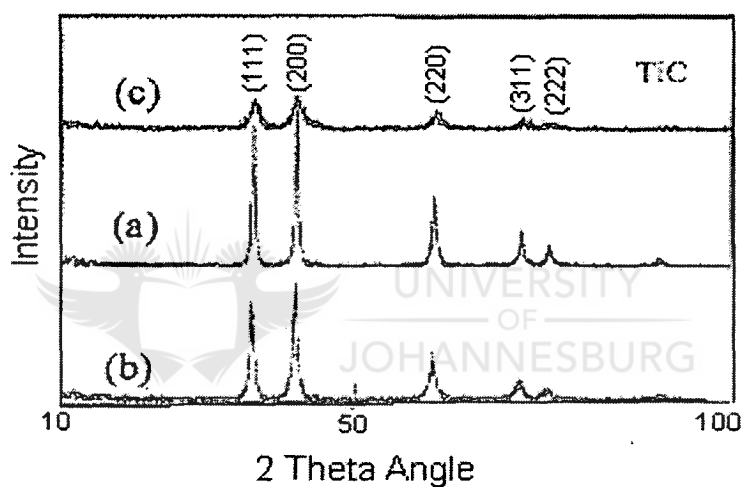
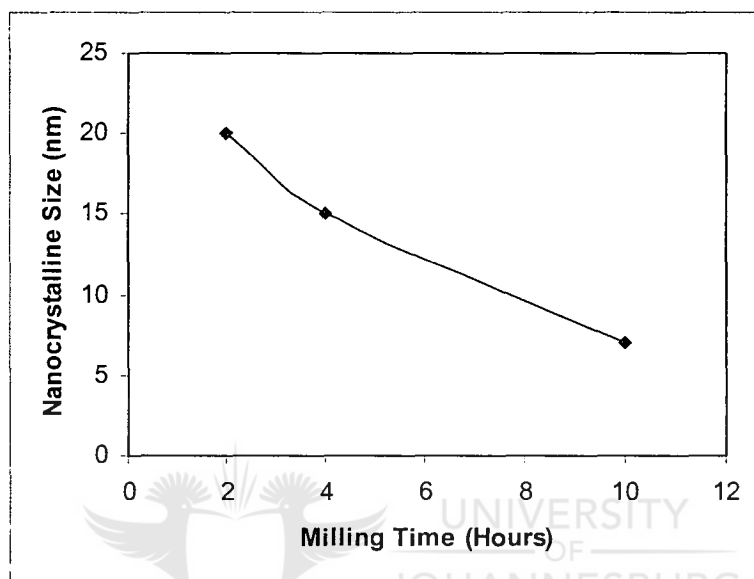


Figure 2.16: XRD spectra of Ti/C (mol) =1:1 at different milling time for (a) 120 min; (b) 240 min; (c) 600 min (Xinkun, 2001).

The longer the milling time is, the wider the peaks of XRD will be. The average crystal size was calculated by Scherrer formula and is shown in figure 2.17. The TiC with 20nm crystallite was produced by ball milling just after reaction in 120 min, with further milling for 600 min crystallite size of 7nm was obtained.



**Figure 2.17:** The relation between nanocrystalline size of TiC powder and milling time (Xinkun, 2001)

**Chapter 3**  
**EXPERIMENTAL**  
**MATERIALS**  
**AND**  
**TECHNIQUES**



### 3.1 Introduction: Powder Preparation

This chapter summarizes the techniques applied in powder preparation route, sintering route and characterisation of carbide and end product.

#### 3.1.1 Mixed Carbide Route

$(\text{Hf}_{0.5}\text{Ti}_{0.5})\text{C}_{0.8}$  was bought from Japan New Metals, some of the powder was milled with 4wt% nickel using for 30 minutes a micronizer mill as shown in figure 3.1. Afterwards a sample was taken for EDS analysis (using a electron microscope) to determine the homogeneity of the mixed powder. Further milling of 1hour was done after the analysis to homogenize the powder further.

#### 3.1.2 Single Carbide Route

Hafnium Carbide (HfC), Titanium Carbide (TiC) and 4%wt Ni were milled in the micronizer mill. First the two carbides were milled together for 2 hrs so as to introduce some defects in the particles for better diffusion then nickel was added and further milling of 2 hrs was done.

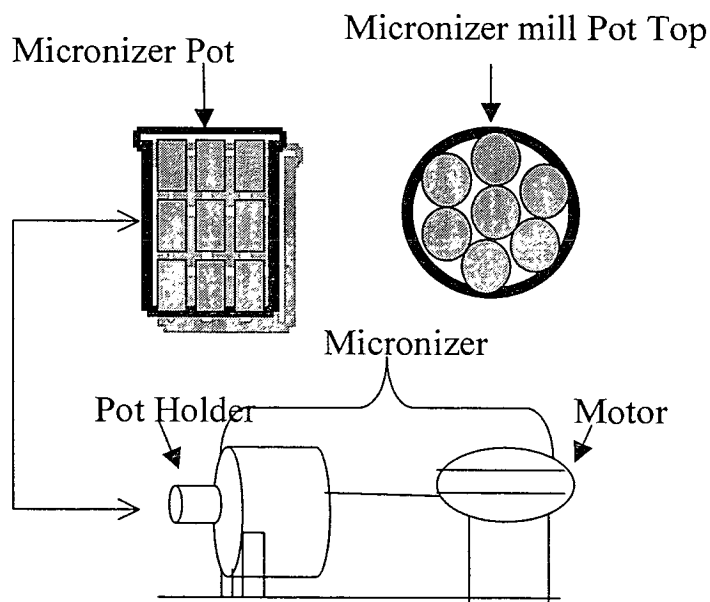
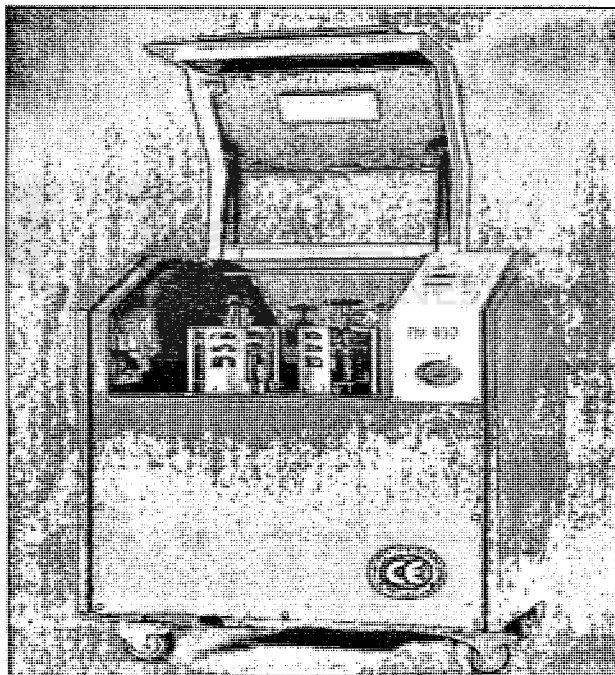


Figure 3.1: Schematic diagram of micronizer mill and its pot

### 3.1.3 Single Carbide Route using high-energy milling

#### 3.1.3.1 Individual milling of HfC and TiC

Hafnium Carbide (HfC) and Titanium Carbide (TiC) were dry milled individually using the high-energy mill Type PM 400 (see figure 3.2). Milling was done for 30 minutes, 1, 2, 3, 4 and 6 hours at a speed of 250 rpm, rotating two ways. Tungsten carbide (WC) balls of 10mm were used as milling media to a 10: 1 ball to powder ratio.



**Figure 3.2:** High-energy mill PM 400/2 (Retsch GmdH, 2000)

### 3.1.3.2 High-energy milling of HfC and TiC together

Hafnium Carbide (HfC) 76wt%, Titanium Carbide (TiC) 22wt% and 2wt% carbon black powder were dry milled in a 250ml pot coated with tungsten carbide with 10mm WC- Co balls as milling media at a rotating speed of 250 rpm rotating two ways (clockwise and anti clockwise) for 12 hrs in air. Some of the high-energy milled powder was then milled in the micronizer mill with 4% wt Ni powder for 4 hrs. Table 3.1 summarises the parameters, which were used for high-energy milling.

**Table 3.1:** Parameters used in High- energy mill

Instrument	Planetary Ball mill, type PM400 (Retsh)
Rotating speed	250rpm
Balls	WC-Co 10 mm (50)
Milling time	12 hrs

## 3.2 Sintering of the Mixed and Single Carbides

Sintering of the carbides was done in a hot press Astro TT HP20-3560-20. The powders were sintered in argon atmosphere but at different temperatures, depending on the presence or absence of nickel.

### 3.2.1 Sintering Mixed and Single Carbide without Nickel

The powder was placed in a graphite pot with a lid as shown in figure 3.3 and sintered at 2000°C. A load of 1100kg was applied corresponding to a pressure of 30 MPa. The load was applied, from 1400°C to 2000°C and pressure removed after sintering.

The pressure was removed before cooling and after sintering the material was furnace cooled. The figure 3.4 and 3.5 shows the sintering cycle.

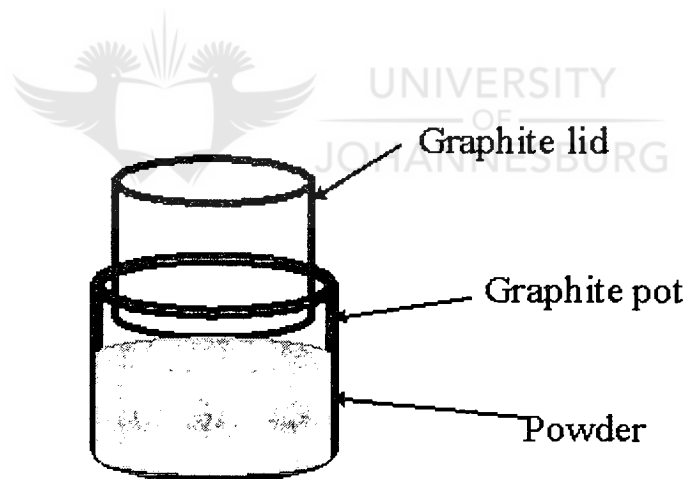


**Figure 3.3:** Schematic of graphite pot in which the powder was placed for Sintering

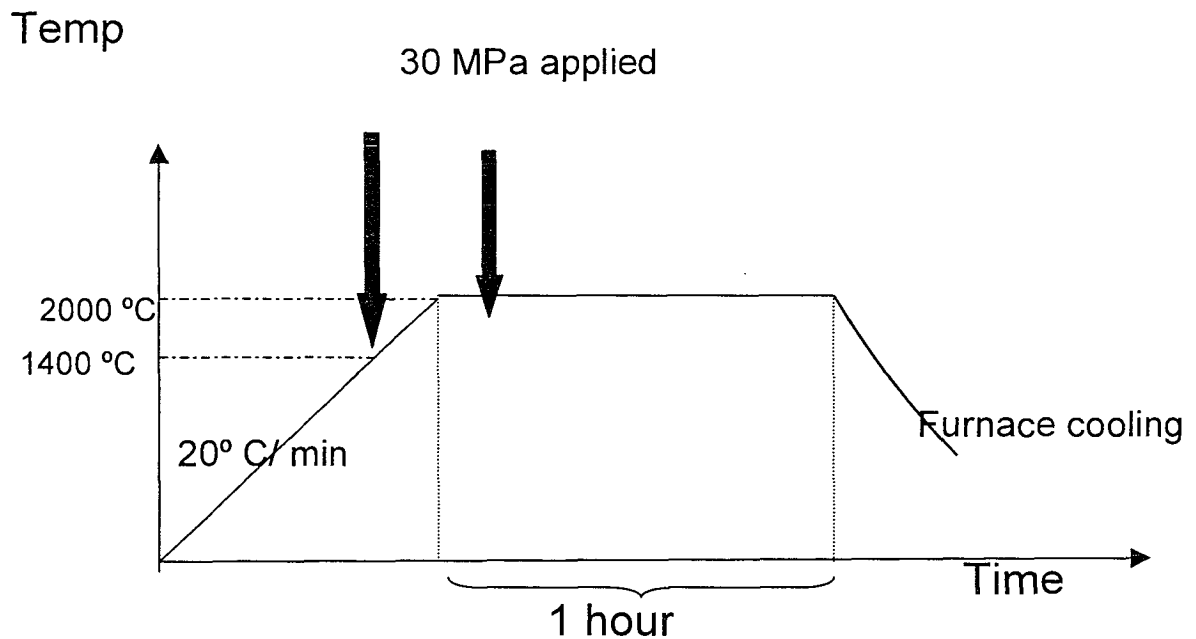


Figure 3.4: Diagram showing the sintering cycle for single and mixed carbide without nickel.

### 3.2.2 Sintering Mixed and Single Carbide with Nickel

The powder was placed in a graphite pot with a lid as shown in figure 3.5 and sintered at 1650°C. A load of 1100kg was applied corresponding to a pressure of 30 MPa. The load was applied from 1100°C to 1650°C and pressure removed after sintering. After sintering, the material was furnace cooled. The graph below shows the sintering cycle.



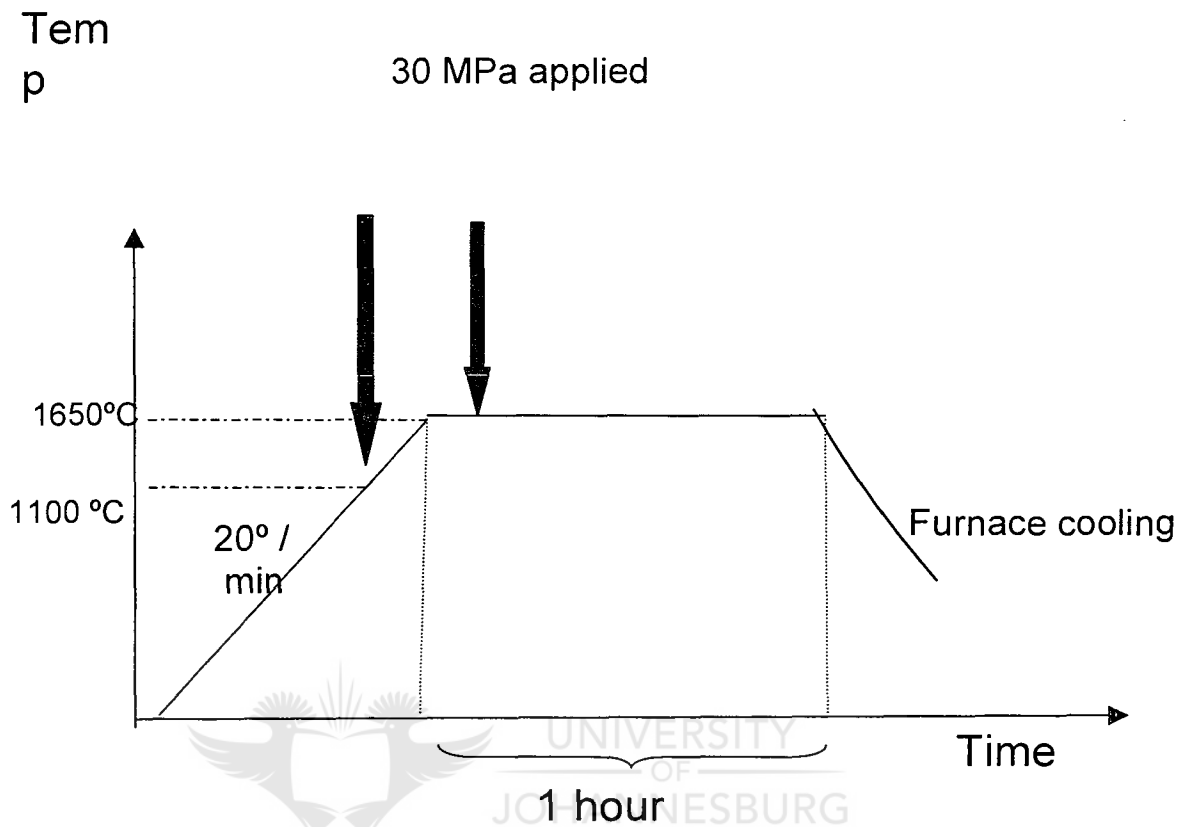


Figure 3.5: Diagram showing the sintering cycle for single and mixed carbide with nickel.

### 3.3 Physical Property Measurements

#### 3.3.1 Particle size Analysis

Particle size analysis was done on all powders received and a MalvernSizer was used for analysis. A small amount of powders were placed in a glass beakers and a small amount of water was added to form a suspension. Then the beaker was placed inside an ultrasonic bath and vibrated for 10 minutes,

in order to break the agglomerates in the powders (some times the ultrasonic probe in the Malvern does not break the agglomerates).

Afterwards a lens is placed into the Malvern, and the bath is cleaned (this should be done every time before using the Malvern because the user before was using a different material).

Then the bath is filled with water, which is done automatically by pressing a clean/fill button on the Malvern. On the Malvern, the pump speed, stirred speed and ultrasonic were adjusted. Afterwards the suspension (powder+ water) is poured into the bath filled with water. Then the computer connected to Malvern is switched on to start measuring particle size. Two measurements can be done on the same material while still in the Malvern, but if left longer the material starts to agglomerate. The table 3.2 below shows the parameters used in the experiment.

**Table 3.2:** Parameters used in particle size analysis

Lens	300 mm
Beam length	2.4 mm
Pump speed	40%
Stirrer speed	80%
Ultrasonic speed	80%

### 3.3.2 Density

The density was measured by using Archimedes Principle; this was done on all sintered specimens, which were prepared from the powders.

- ❖ Mass of the dry sample was measured
- ❖ A glass beaker was filled with tap water and samples to be measured put inside
- ❖ The samples were boiled for 1 hour and after the water was let to cool at room temperature
- ❖ The suspended mass of samples in water was measured
- ❖ The sample was dried on the outside using a towel (but care must be taken in drying the samples not too dry)
- ❖ Mass after drying was measured

A following formula was used to calculate the Bulk density:

$$\text{Bulk density } \delta = \frac{d\delta(H_2O)}{(we - w)}$$
$$\text{Open Porosity } Po = \frac{(we - d)}{\delta(H_2O)V}$$
$$= 100\% (we - d)/(we - w)$$

$\delta$ = density of water

$d$ = dry mass of sample

$we$ = mass of wet sample

$w$ = mass of sample in water

### 3.3.3 Preparation of sintered specimens for metallographic analysis

Sintered specimens were cut into four pieces using a diamond wheel and were mounted in resin. The surfaces were ground flat using a 6 $\mu$ m diamond paste on a reserved cloth with lubricant and further polishing was done with reserved cloth and diamond spray of 1 $\mu$ m until a reflecting surface was obtained on the ceramic material.

## 3.4 Mechanical property measurements

### 3.4.1 Vickers hardness

Vickers hardness values were measured by driving a pyramidal Vickers diamond indenter into polished specimens surface at a load of 1, 10 and 30kg. The size of the indentation was measured under an optical microscope (measuring the diagonals). The hardness values were calculated from a minimum of 3 indentations in each of the samples and each load.

The equation for Vickers hardness is the following:

$$H_v = \frac{P \times 1.85}{d^2}$$

P= Load applied in kg

D=Diagonal in mm

Hv= Vickers hardness

UNIVERSITY  
OF  
JOHANNESBURG

### 3.4.2 Scanning electron microscopy (SEM)

The specimens which were polished were then carbon coated and investigated by SEM. EDS was used in combination with SEM analysis to identify which elements are present in the materials. EDS was also used to analyze the powders before sintering to assess their homogeneity. Also quantitative analysis was done the Japan New Metal sintered materials with and without Ni.

### 3.4.3 XRD (x-ray diffraction)


XRD (x-ray diffraction) was used to analyse the phases in the powders and sintered materials. Table 3.3 below shows the parameters which were used for analysis

**Table 3.3:** Parameters which were used for XRD analysis

Instrument	
Scan step	0.02
Time per step	3
Scan type	Continuous
Angels Scanned $2\theta$	20- 80°
Anode material	Cu $K_{\alpha}$
Generator voltage	40 kv
Tube current	45 Am
Wavelength	0.154056 nm
Monochromatic used	Yes

The powder and sintered materials were prepared by placing them in a platinum holder. The powder has to be level to the top surface of the holder. When starting the analysis, precautions must be taken to check that the shutter is open and high tension kV and current mA are at 40 and 20. After analysis, the powder was stored separately from the other powder for future use.

**Chapter 4**  
**EXPERIMENTAL RESULTS**  
**AND**  
**DISCUSSION**

The image shows a chapter title page for Chapter 4. The text is centered and reads "Chapter 4", "EXPERIMENTAL RESULTS", "AND", and "DISCUSSION". A watermark of the University of Johannesburg logo is visible in the background, featuring two stylized figures holding hands above an open book, with the text "UNIVERSITY OF JOHANNESBURG" below it.

## 4. Introduction

This chapter summarizes the results obtained by applying the techniques described in chapter 3. The results have been divided into 6 sections:

- 1) The characterization of as received powders
- 2) The characterization of high-energy dry milled individual powders
- 3) The characterization of high-energy dry milled carbides mixture
- 4) The characterization sintered pre-reacted  $(\text{Hf}_{0.5}\text{Ti}_{0.5})\text{C}_{0.8}$  with and without binder
- 5) The characterization sintered mixed (not milled)  $\text{HfC} + \text{TiC}$  with binder
- 6) The characterization sintered high-energy milled  $\text{HfC} + \text{TiC} + \text{C}$  powder with and without binder



## 4.1 Characterization of the as received powders

This section includes results obtained from XRD analysis, SEM and EDS analysis of the  $(\text{Hf}_{0.5}\text{Ti}_{0.5})\text{C}_{0.8}$ , TiC and HfC as they were received.

### 4.1.1 Powder characterization by XRD

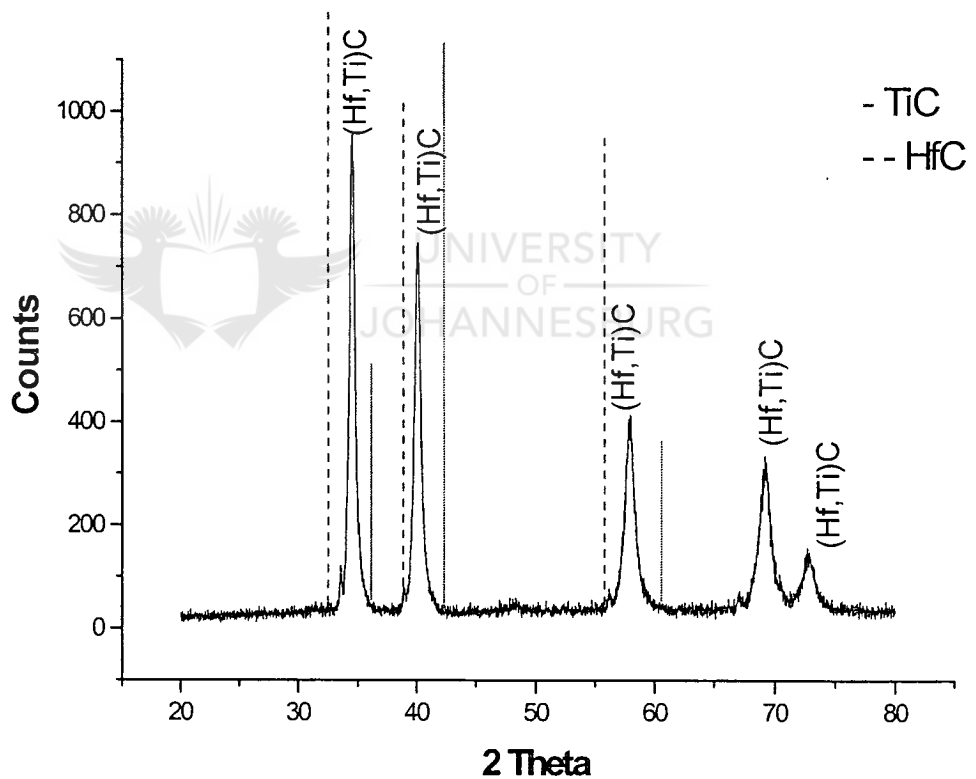


**Figure 4.1:** XRD results of  $(\text{Hf}_{0.5}\text{Ti}_{0.5})\text{C}_{0.8}$  powder from Japan New Metals. The dash and dot lines show the expected position of the HfC and TiC peaks respectively. See Appendix 1 for the d-values.



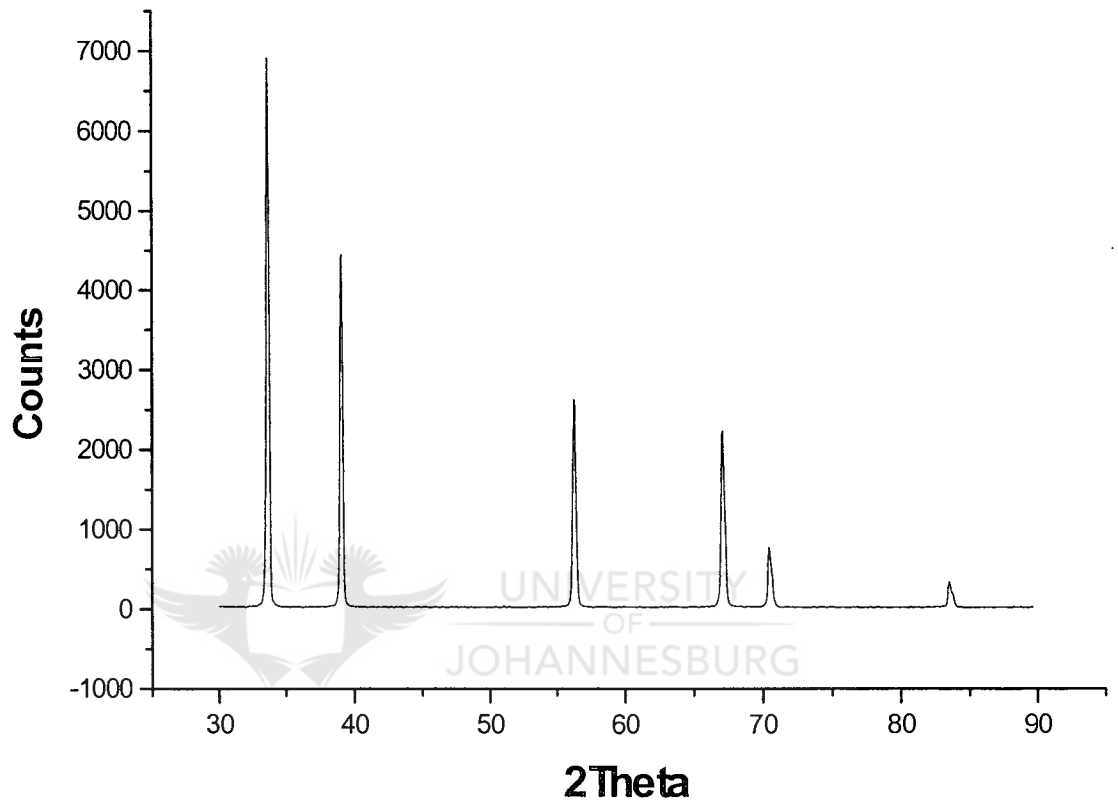


**Figure 4.2:** XRD results of HfC powder from Japan New Metals  
See Appendix 1 for the d-values.

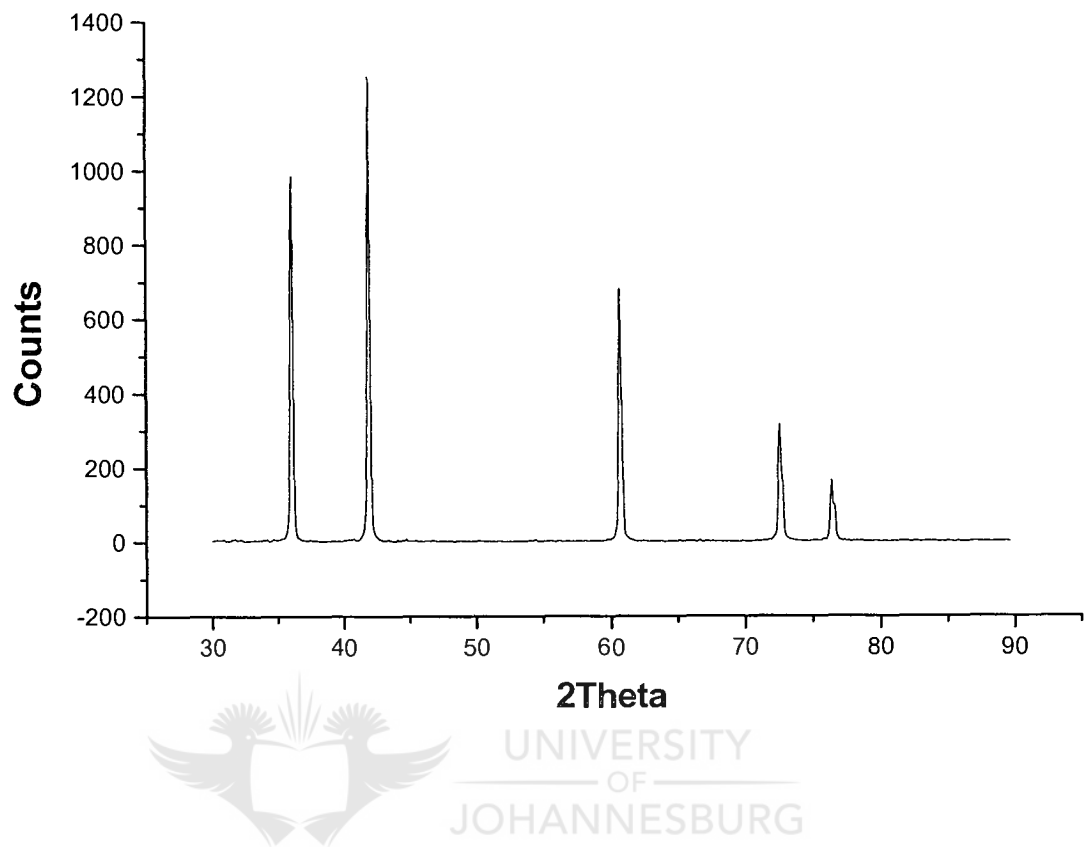


**Figure 4.3:** XRD results of TiC powder Goodfellow Metals.

See Appendix 1 for the d-values.

#### 4.1.2 SEM Micrographs of powders

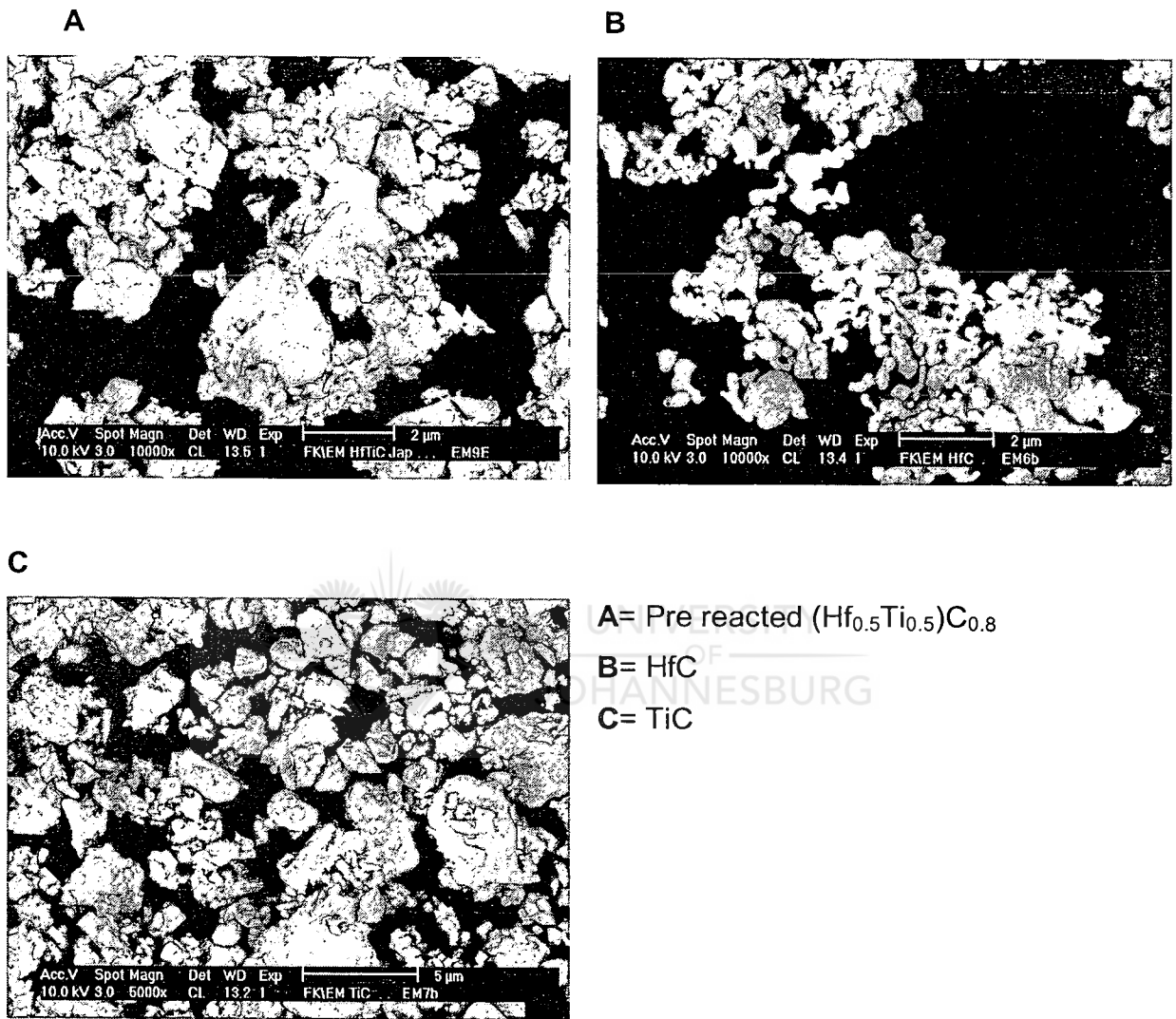


Figure 4.4: SEM micrographs of the powders as received from suppliers

#### 4.1.3 Particle size analysis results of received powders by MalvernSizer

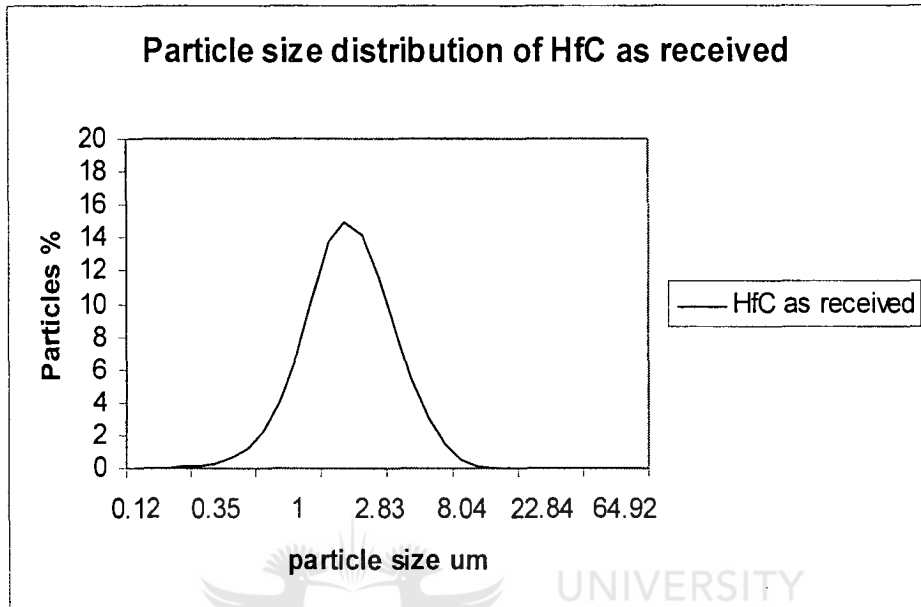


Figure 4.5: Particle size analysis of the HfC powder as received (See Appendix 4)

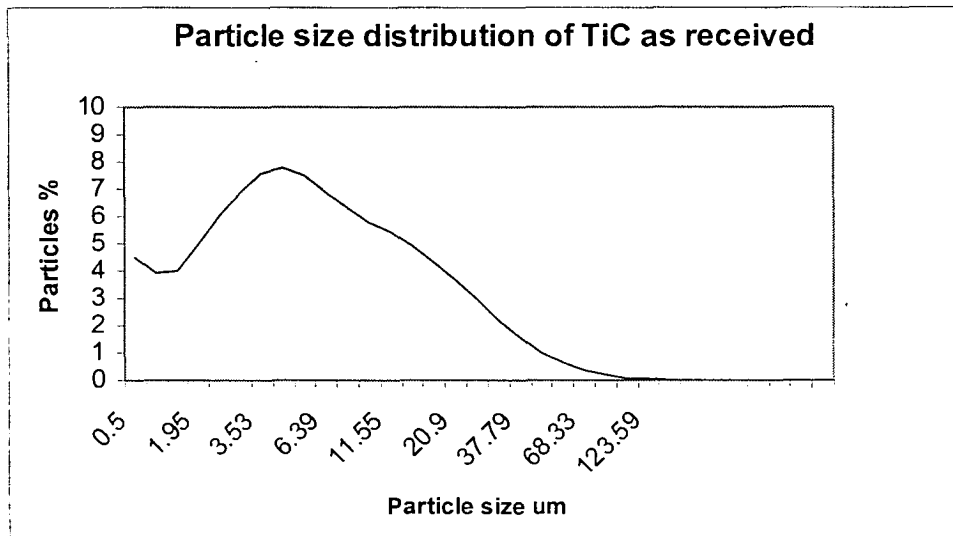


Figure 4.6: Particle size analysis of the TiC powder as received (See Appendix 7)

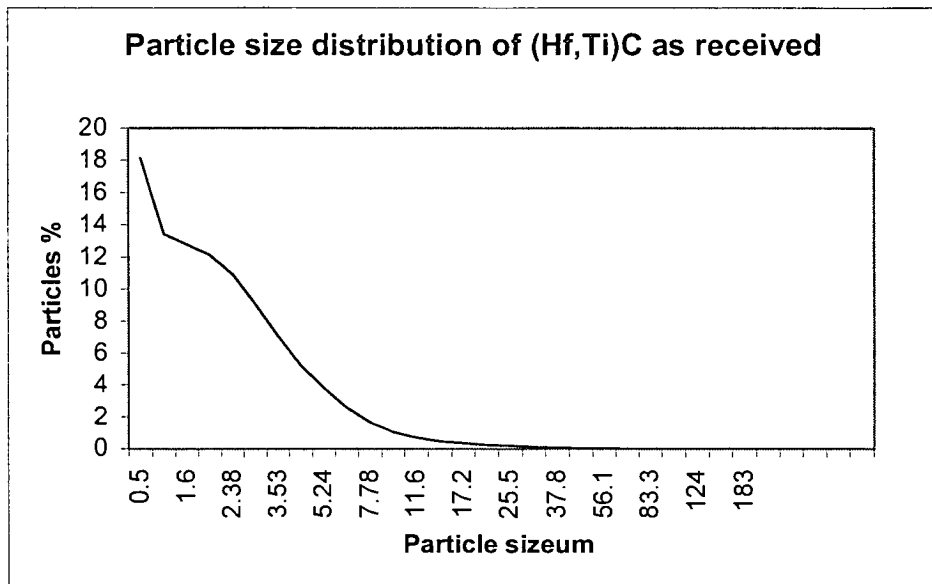


Figure 4.7: Particle size analysis of the  $(\text{Hf}_{0.5}\text{Ti}_{0.5})\text{C}_{0.8}$  as received powder

(See Appendix 10)



4.1.4 EDS results from the  $(\text{Hf}_{0.5}\text{Ti}_{0.5})\text{C}_{0.8}$  powder

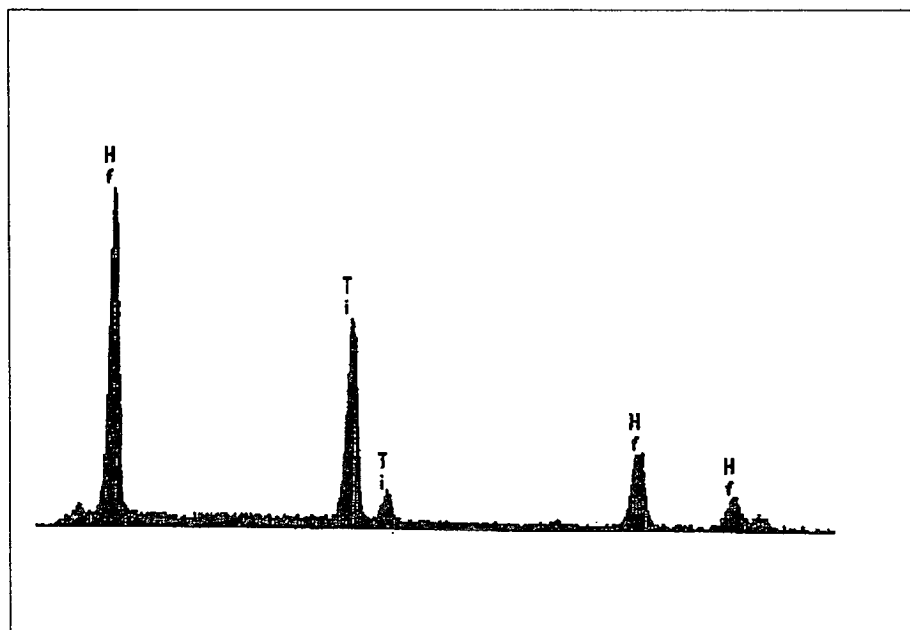


Figure 4.8: EDS spectrum of the  $(\text{Hf}_{0.5}\text{Ti}_{0.5})\text{C}_{0.8}$  powder

#### 4.1.5 Discussion

Powders were characterized as received, by SEM, XRD, EDS and Malvern particle size analysis. These analyses were done to determine the phases present and the particle size. From figure 4.1 the XRD results from  $(\text{Hf}_{0.5}\text{Ti}_{0.5})\text{C}_{0.8}$  show that the material received is a solid solution of HfC and TiC because the XRD peaks of this material are between those of the two carbides. The powder appears to consist of a range of compositions, as suggested by the width of the peaks.

According to literature the  $\text{TiC}_y$  lattice parameter of 0.43 nm (which was obtained the d-values is Appendix 1 corresponds to  $y \approx 0.73$  and the  $\text{HfC}_z$  lattice parameter of 0.46 nm (also obtained from the d-values) corresponds to  $z \approx 0.75$ . Therefore, in both as received single carbide powders the C/M (M-metal) ratio was markedly lower than the ratio at which the hardness of the carbides is reported to the highest namely  $\text{C/M} \approx 0.95$  (Ramqvist, 1969). As for the (Hf, Ti) C powder although its nominal formula (i.e the formula given by the suppliers was  $(\text{Hf}_{0.5}\text{Ti}_{0.5})\text{C}_{0.8}$ . According to Perry, (1987) the lattice parameter of 0.45 corresponds to Hf/Ti molar ratio of approximately 60/40 and not 50/50. But the lattice parameter depends also on the carbon content and the analytical techniques determine the C content, so The analytical techniques available for this investigation did not allow to confirm that actually the formula of  $(\text{Hf}_{0.5}\text{Ti}_{0.5})\text{C}_{0.8}$  powder was the nominal one.

The XRD results in Figures 4.2 and 4.3 show that the materials characterized are HfC and TiC and they are crystalline. The Malvern results show that the particle size of the powders had a wide distribution. HfC showed the average particle size of 2.18  $\mu\text{m}$ , TiC average particle size of 5.77  $\mu\text{m}$  and  $(\text{Hf}_{0.5}\text{Ti}_{0.5})\text{C}_{0.8}$  average particle size of 2.14  $\mu\text{m}$ .

## 4.2. Characterization of high-energy milled individual carbide powders (HfC and TiC).

These powders were characterized by XRD and Malvern analysis

### 4.2.1 Individual milling of HfC

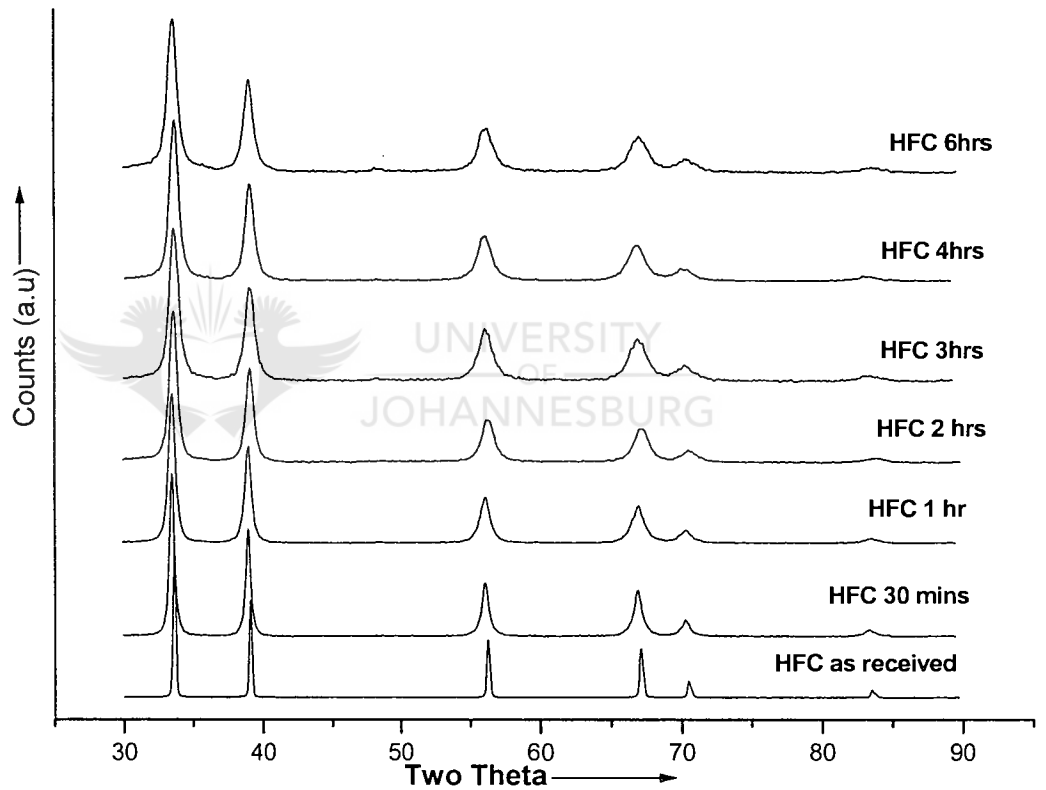


**Figure 4.9:** XRD results of individually milled HfC powder from Japan New Metals. Samples were analysed after 30 mins, 1,2,3,4 and 6 hours of milling

## 4.2.2 Individual milling of TiC

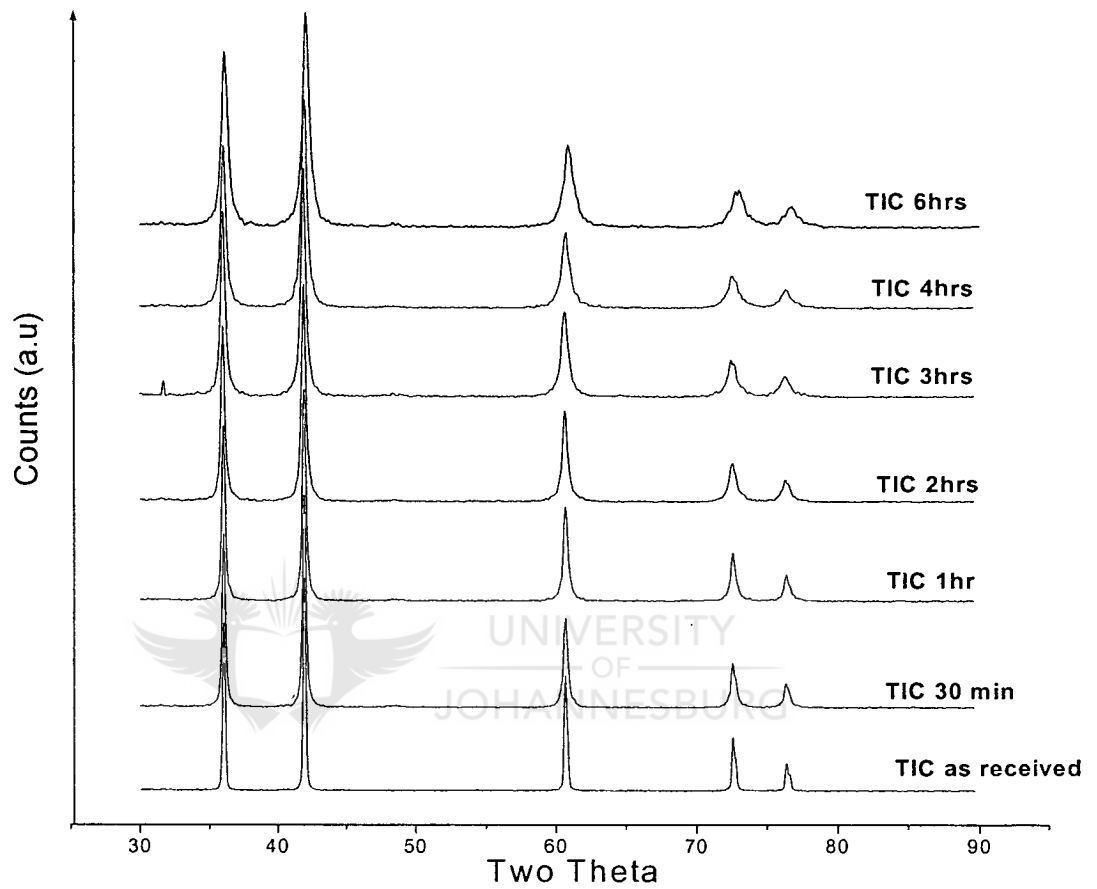


Figure 4.10: XRD results of TiC powder individually milled.



#### 4.2.3 Particle size analysis by MalvernSizer of HfC powders after high-energy milling

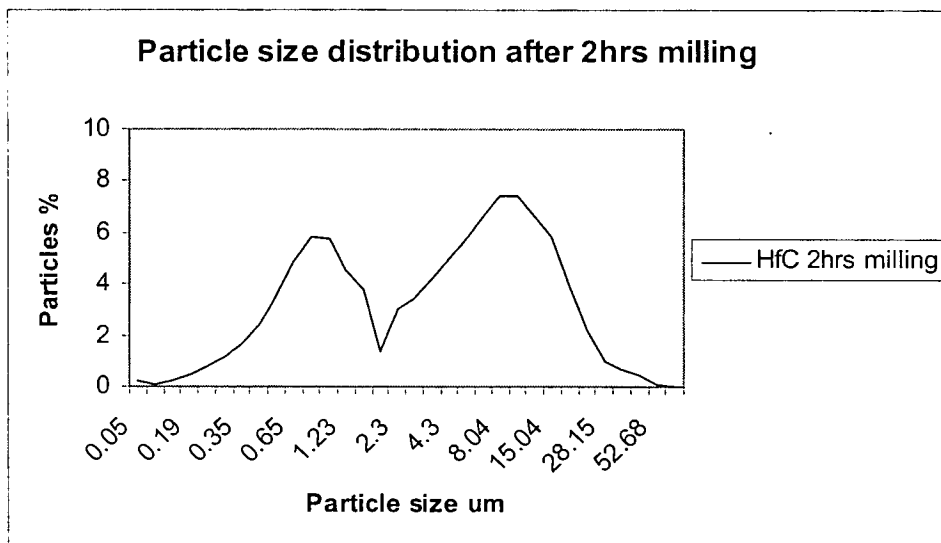


Figure 4.11: Particle size analysis showing change in particle size of HfC powder after 2 hours of high- energy milling (See Appendix 5)

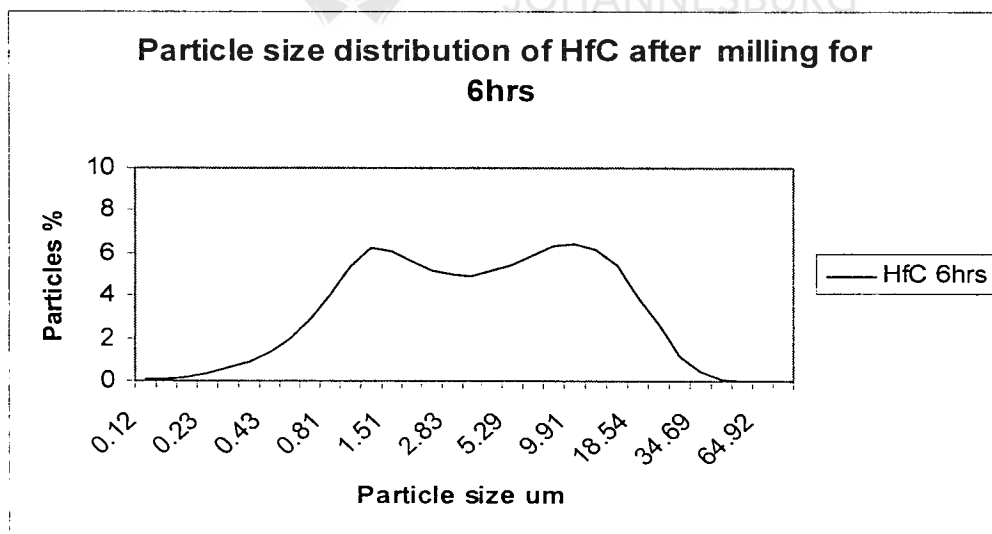


Figure 4.12: Particle size analysis showing change in particle size of HfC powder after 6 hours of high- energy milling (See Appendix 6)

#### 4.2.4 Particle size analysis by MalvernSizer of TiC powders after high-energy milling

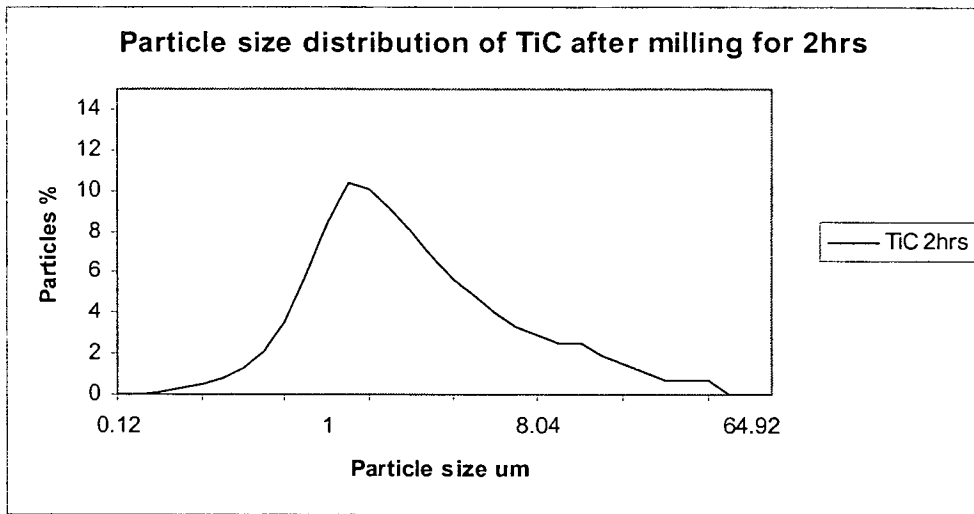


Figure 4.13: Particle size analysis showing change in particle size of TiC powder after 2hrs of high- energy milling (See Appendix 8)

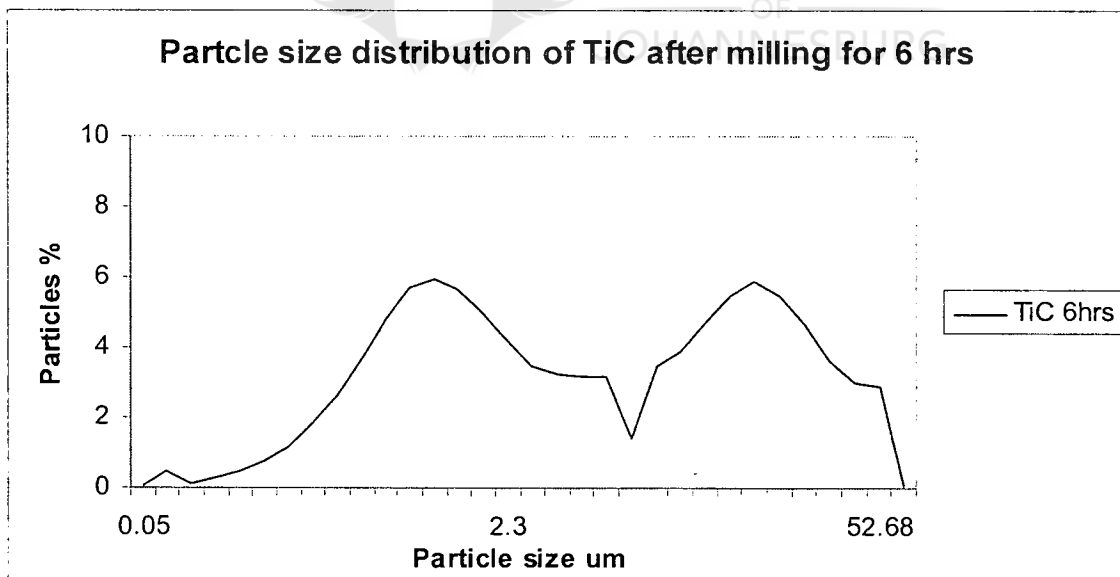


Figure 4.14: Particle size analysis showing change in particle size of TiC powder after 6hrs of high- energy milling (See Appendix 9)

## 4.2.5 d-values of HfC and TiC after every high-energy milling

Table 4.1: HfC d-values vs milling time

Hours	d- values		
<b>Theoretical values</b>	<b>2.6776</b>	<b>2.3189</b>	<b>1.6400</b>
<b>As received</b>	2.6609	2.3061	1.6342
<b>30 min</b>	2.6661	2.3098	1.6369
<b>1</b>	2.6649	2.3071	1.6349
<b>2</b>	2.6604	2.3077	1.6378
<b>3</b>	2.6657	2.3154	1.6316
<b>4</b>	2.6637	2.3083	1.6342
<b>6</b>	2.6629	2.3119	1.6446



Table 4.2: TiC d-values vs milling time

Hours	d- values		
<b>Theoretical values</b>	<b>2.50</b>	<b>2.16</b>	<b>1.53</b>
<b>As received</b>	2.4872	2.1544	1.526
<b>30 min</b>	2.4877	2.1536	1.5249
<b>1</b>	2.4872	2.1546	1.5261
<b>2</b>	2.4882	2.1558	1.5257
<b>3</b>	2.4886	2.1550	1.5249
<b>4</b>	2.4843	2.1540	1.5236
<b>6</b>	2.4867	2.1533	1.5276

#### 4.2.6 Results of grain size and strain in high-energy milled HfC and TiC (calculated by the Rietveld Method; IKTS):

**Table 4.3:** Results of grain size and strain in HfC and TiC (Rietveld Method; IKTS):

Conditions	HfC		TiC	
	D,nm	Strain	D,nm	Strain
0 h	>150	0	>150	0
2 h	36 ± 4	1 x 10 <sup>-2</sup>	42 ± 4	7 x 10 <sup>-2</sup>
6 h	20 ± 4	8 x 10 <sup>-2</sup>	36 ± 4	8 x 10 <sup>-2</sup>



#### 4.2.7 Summary of result 4.2.1 to 4.2.6

The individual dry milling of HfC and TiC was done for 0.5,1,2,3,4 and 6 hour(s) to establish how these powders behave during high energy milling. XRD analysis was done on each material after milling and the results can be seen in Figure 4.9 and 4.10. These results show a broadening of peaks as milling time increases which shows the reduction in particle size. The particle size was calculated using the Rietveld method and results are shown in table 4.3, showing that part of the broadening was due to strain.

The d-values of the XRD peaks showed some decrease and this is expected to be due to carbon loss during milling. Results in Tables 4.1 and 4.2 show increase and decrease in d-values, because after every milling a new powder was used. Particle size was also measured using Malvern analyser and it was seen that in Figure 4.11, 4.12, 4.13 and 4.14 there was reduction in particle size as confirmed in table 4.3 and bimodal- agglomerates were observed (see appendix i-vii) during high energy milling. This could be due to the welding of particles together during milling (Benjamin, 1983).

### 4.3 Characterization of high-energy dry milled carbide mixture.

The mixture that was high-energy milled consisted of 22 wt% TiC, 76 wt % HfC and 2 wt %C. The mixed powder was characterized by XRD, SEM, EDS and Malvern analysis.

#### 4.3.1 XRD results of high- energy dry milling of carbide mixture

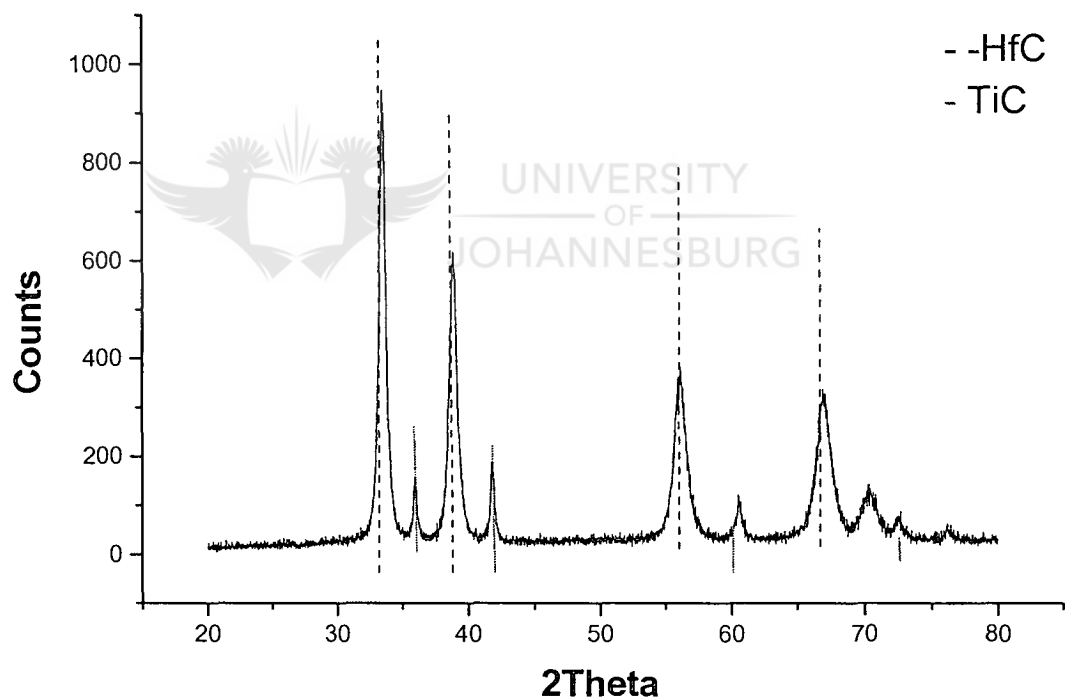
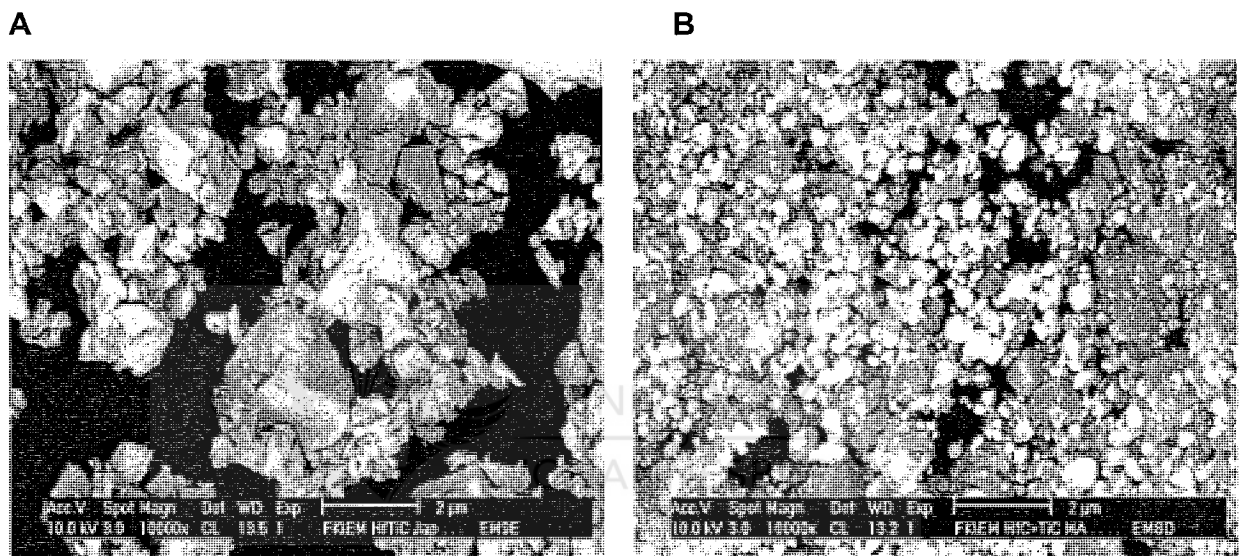


**Figure 4.15:** XRD results of HfC+TiC+ carbon black mixed powder after high- energy dry milling for 12 hrs. The dash and dot lines represent the positions predicted by the literature for the peaks of HfC and TiC respectively

### 4.3.2 Examination by SEM



A=  $(\text{Hf}_{0.5}\text{Ti}_{0.5})\text{C}_{0.8}$

B= HfC +TiC high-energy milled

**Figure 4.16:** SEM micrographs of the  $(\text{Hf}_{0.5}\text{Ti}_{0.5})\text{C}_{0.8}$  as received powder and the high-energy dry milled HfC +TiC+ carbon black powder

### 4.3.3 Examples of EDS results HfC +TiC+C powder after high-energy dry milling for 12 hrs

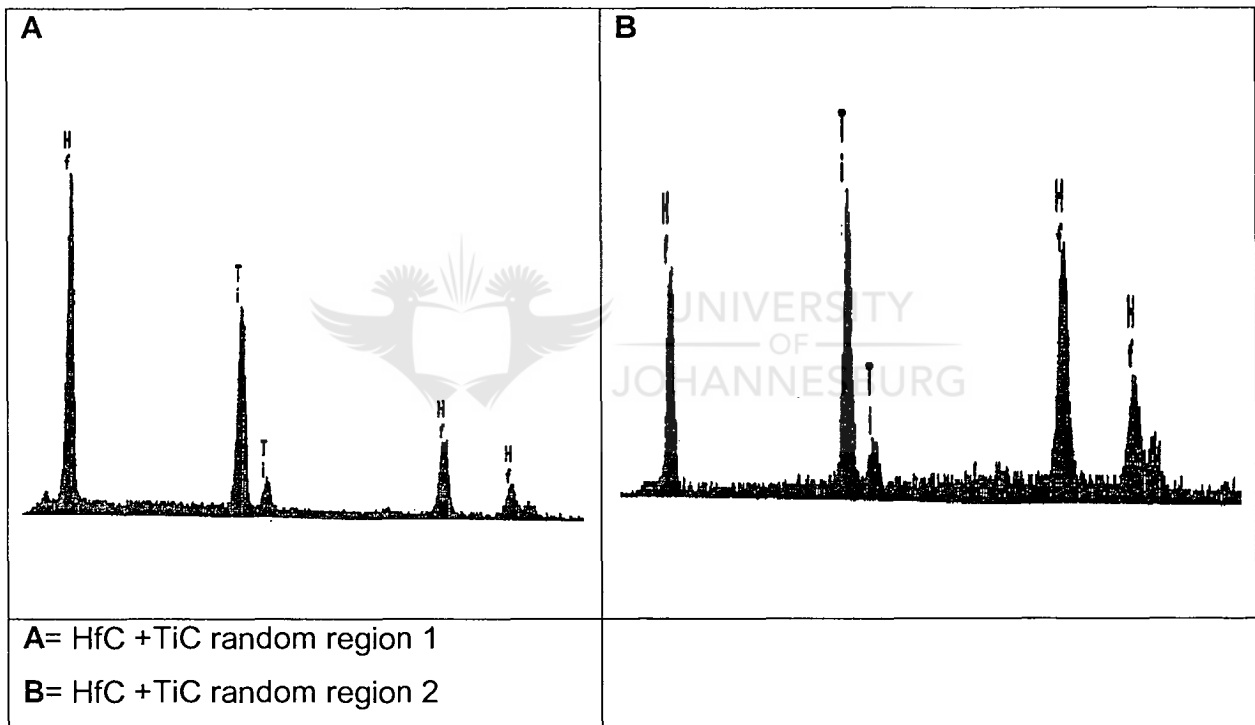


Figure 4.17: EDS spectra of HfC +TiC after high- energy dry milled for 12 hrs, from two random regions, showing obvious difference in composition.



4.3.4 Particle size analysis by MalvernSizer of HfC+TiC powder after high-energy dry milling

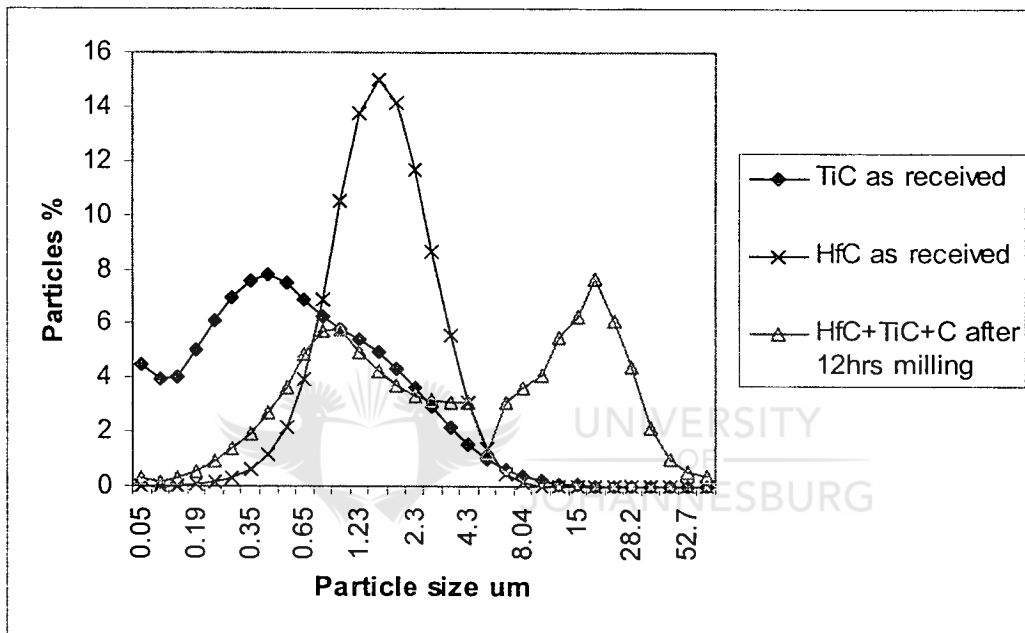
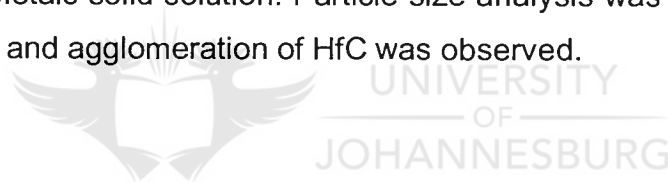


Figure 4.18: Particle size analysis showing particle size of HfC +TiC + carbon black powder after high- energy milling for 12 hours (See Appendix 11)

### 4.3.5 Summary of results from 4.3.1 to 4.3.4

A powder consisting of 76 wt %HfC, 22 wt %TiC and 2 wt % carbon black was milled for 12 hours in the high-energy mill PM400/2 in air. Carbon black was added in order to compensate for carbon loss during milling and for the substoichiometry of the HfC and TiC powders. The aim of this was to produce a mixed carbide having the same composition as  $(\text{Hf}_{0.5}\text{Ti}_{0.5})\text{C}_{0.8}$ , and compare the materials produced from the two different powders.

XRD was done on the powder after milling to know if a solid solution was formed during milling. The results in figure 4.15 showed that there was a small shift in the HfC, TiC peaks but a solid solution was not formed. This can be also seen in figure 4.16B, where this powder was compared to the (Hf,Ti)C Japan New Metals solid solution. Particle size analysis was done, results are in figure 4.18 and agglomeration of HfC was observed.



#### 4.4 Characterization of sintered samples produced from the $(\text{Hf}_{0.5}\text{Ti}_{0.5})\text{C}_{0.8}$ pre-reacted powders

Samples were produced with and without Ni binder. They were hot pressed at 30 MPa.

##### 4.4.1 XRD results from sintered pre- reacted $(\text{Hf}_{0.5}\text{Ti}_{0.5})\text{C}_{0.8}$ powder without Ni

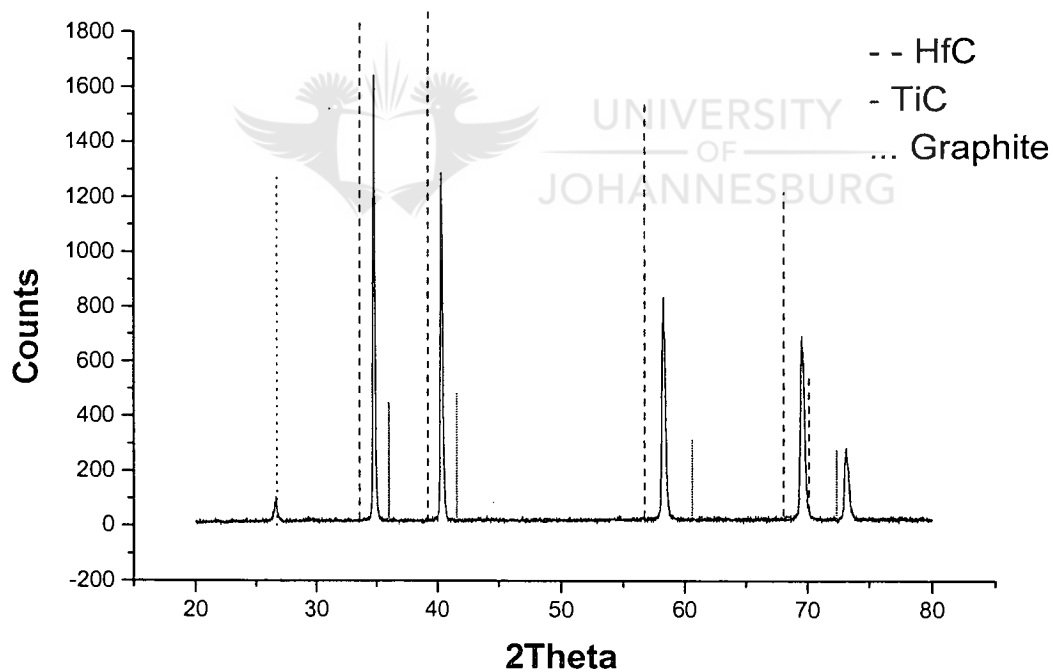


**Figure 4.19:** XRD results from  $(\text{Hf}_{0.5}\text{Ti}_{0.5})\text{C}_{0.8}$  hot pressed at 2000°C and 30 mPa. The d-values are in Appendix 2. The graphite peak was a residue from the graphite box in which the materials were hot pressed.

#### 4.4.2 XRD results from sintered pre- reacted $(\text{Hf}_{0.5}\text{Ti}_{0.5})\text{C}_{0.8}$ powders with 4 wt %Ni

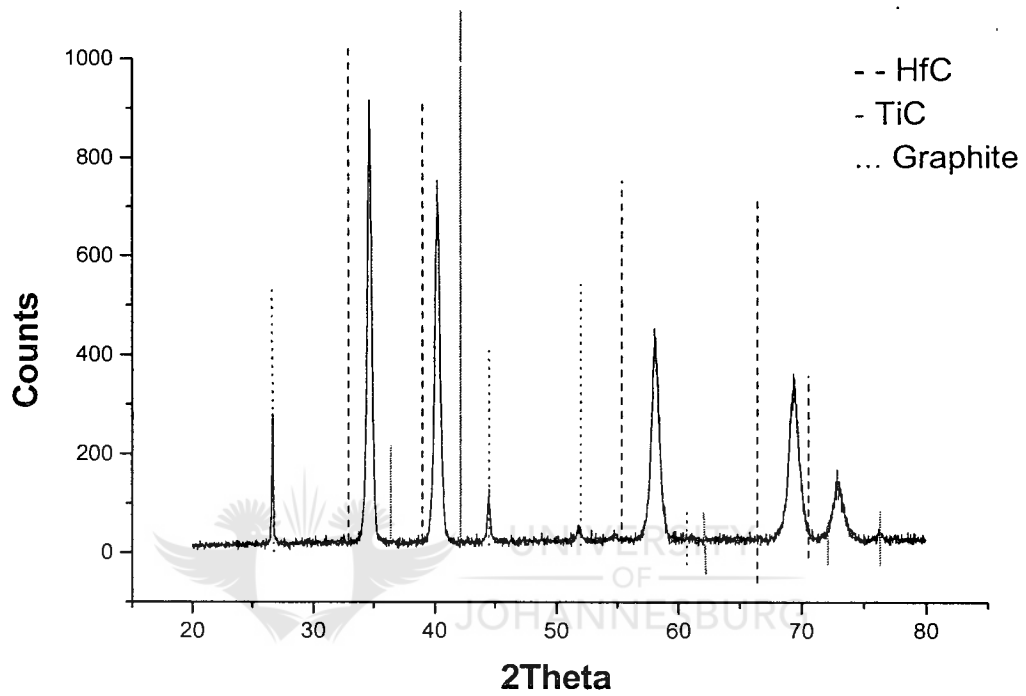


**Figure 4.20:** XRD results from  $(\text{Hf}_{0.5}\text{Ti}_{0.5})\text{C}_{0.8} + 4\%$  Ni hot pressed at  $1650^{\circ}\text{C}$  and 30 MPa. Ni peaks could not be identified. The d-values are in Appendix 2.

#### 4.4.3 EDS results from polished surfaces

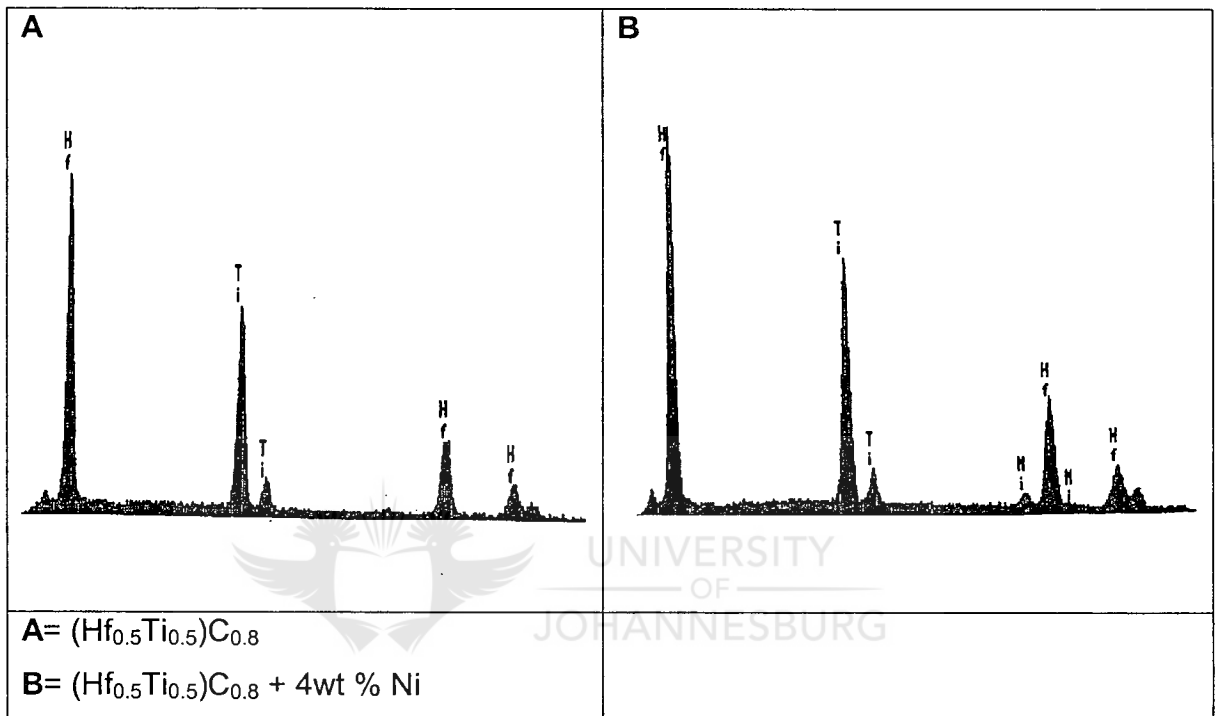
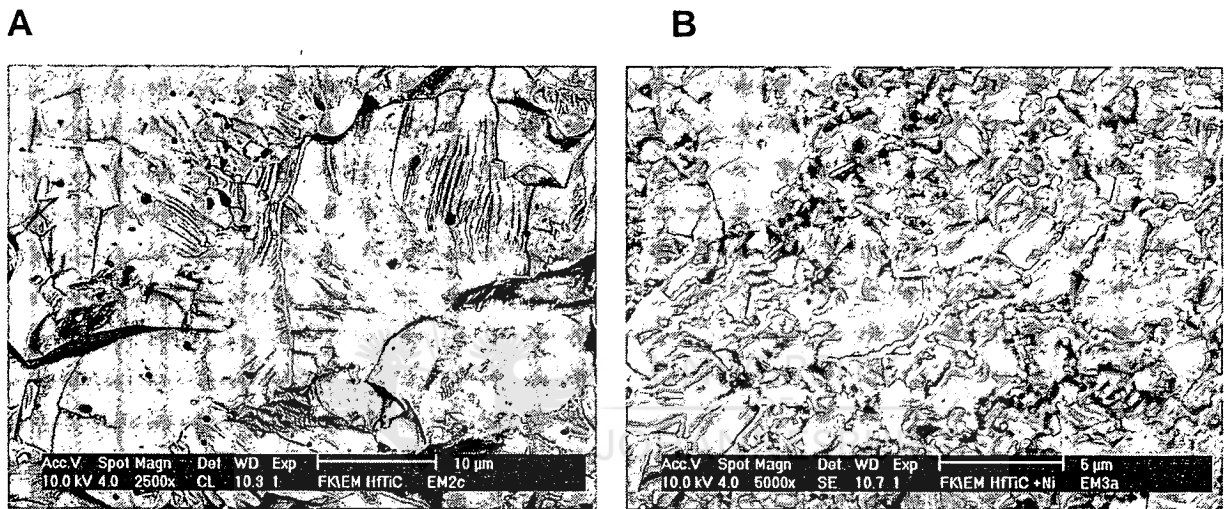


Figure 4.21: EDS spectra on  $(\text{Hf}_{0.5}\text{Ti}_{0.5})\text{C}_{0.8}$  and  $(\text{Hf}_{0.5}\text{Ti}_{0.5})\text{C}_{0.8} + 4\% \text{ Ni}$  polished surfaces

#### 4.4.4 SEM Micrographs of sintered $(\text{Hf}_{0.5}\text{Ti}_{0.5})\text{C}_{0.8}$ and of sintered $(\text{Hf}_{0.5}\text{Ti}_{0.5})\text{C}_{0.8} + \text{Ni}$ fracture surfaces



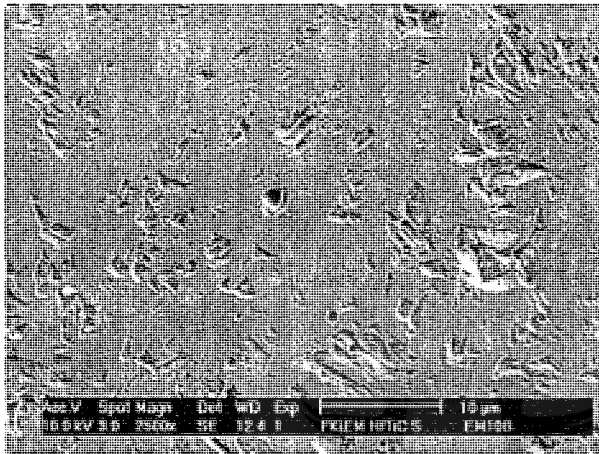
A=  $(\text{Hf}_{0.5}\text{Ti}_{0.5})\text{C}_0$ .

B=  $(\text{Hf}_{0.5}\text{Ti}_{0.5})\text{C}_{0.8} + 4 \text{ wt\% Ni}$

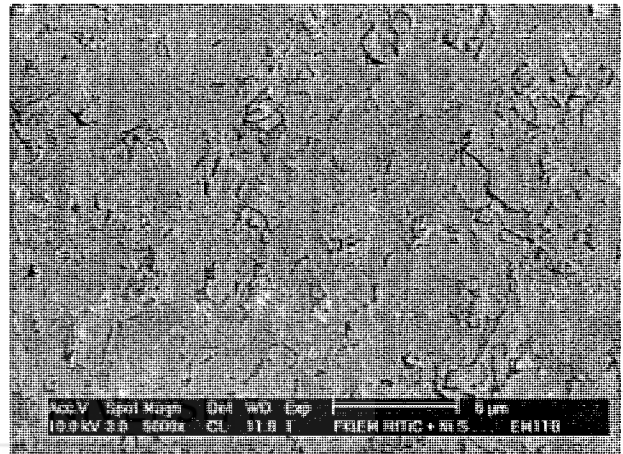
Figure 4.22: SEM micrographs of sintered  $(\text{Hf}_{0.5}\text{Ti}_{0.5})\text{C}_{0.8}$  and of sintered  $(\text{Hf}_{0.5}\text{Ti}_{0.5})\text{C}_{0.8} + \text{Ni}$  fracture surfaces

#### 4.4.5 SEM micrographs of sintered $(\text{Hf}_{0.5}\text{Ti}_{0.5})\text{C}_{0.8}$ and sintered $(\text{Hf}_{0.5}\text{Ti}_{0.5})\text{C}_{0.8} + \text{Ni}$ polished surfaces

A



B



A=  $(\text{Hf}_{0.5}\text{Ti}_{0.5})\text{C}_0$ .

B=  $(\text{Hf}_{0.5}\text{Ti}_{0.5})\text{C}_{0.8} + 4\text{wt}\% \text{ Ni}$

Figure 4.23: SEM Micrographs of sintered  $(\text{Hf}_{0.5}\text{Ti}_{0.5})\text{C}_{0.8}$  and of sintered  $(\text{Hf}_{0.5}\text{Ti}_{0.5})\text{C}_{0.8} + \text{Ni}$  polished surfaces





#### 4.4.6 Density measurements of sintered $(\text{Hf}_{0.5}\text{Ti}_{0.5})\text{C}_{0.8}$ and of sintered $(\text{Hf}_{0.5}\text{Ti}_{0.5})\text{C}_{0.8} + 4 \text{ wt \% Ni}$

**Table 4.4:** Density of sintered  $(\text{Hf}_{0.5}\text{Ti}_{0.5})\text{C}_{0.8}$  and of sintered  $(\text{Hf}_{0.5}\text{Ti}_{0.5})\text{C}_{0.8} + 4\text{wt\% Ni}$

Material	Density
Theoretical density	9.36 g/cm <sup>3</sup>
$(\text{Hf}_{0.5}\text{Ti}_{0.5})\text{C}_{0.8}$	9.17 g/cm <sup>3</sup>
$(\text{Hf}_{0.5}\text{Ti}_{0.5})\text{C}_{0.8} + \text{Ni}$	9.19 g/cm <sup>3</sup>

#### 4.4.7 Hardness Results

**Table 4.5:** Vickers Hardness of sintered  $(\text{Hf}_{0.5}\text{Ti}_{0.5})\text{C}_{0.8}$  and of sintered  $(\text{Hf}_{0.5}\text{Ti}_{0.5})\text{C}_{0.8} + 4 \text{ wt \% Ni}$

Load	$(\text{Hf}_{0.5}\text{Ti}_{0.5})\text{C}_{0.8}$ Sintered at 2000°C	$(\text{Hf}_{0.5}\text{Ti}_{0.5})\text{C}_{0.8} + 4\%$ Ni Sintered at 1650°C
1kg	2055 Hv	2737 Hv
5kg	Brittle*	2330 Hv
10kg	Brittle*	2335 Hv
30kg	Brittle*	2195 Hv

\* too brittle to measure hardness by Vickers method.

#### 4.4.8 Discussion

The pre- alloyed  $(\text{Hf}_{0.5}\text{Ti}_{0.5})\text{C}_{0.8}$  powder and the  $(\text{Hf}_{0.5}\text{Ti}_{0.5})\text{C}_{0.8} + 4 \text{ wt \%Ni}$  powder were sintered. The powders were not homogeneous and the system tended to homogenize as shown in figure 4.19 and 4.20 by the narrowing of XRD peaks after sintering (compared with figure 4.1). The width of the XRD peaks decreased slightly after sintering at  $1650^{\circ}\text{C}$  but decreased significantly after sintering at  $2000^{\circ}\text{C}$  suggesting progressive homogenization and could also result from grain growth with increased crystallinity.

In the presence of Ni, sintering occurred with the formation of a liquid phase. The volume fraction of liquid formed was sufficient to yield a low porosity. Grain growth was less in figure 4.22B than in case of material sintered without Ni (shown in figure 4.22A), probably just on account of the lower sintering temperature. The density of the materials measured was above 95% (shown in table 4.4) of the theoretical density which suggest the presence of only close porosity. On the fracture surface of the binderless material the pores are  $1\text{-}2\mu\text{m}$  in size and mostly within the grains. The pores appear to be consistent with sintering occurring through inter-diffusion of Hf and Ti atoms from and into (Hf,Ti)C particles of unequal composition and at different diffusion rate.

The hardness of both with- binder and binder-less materials is lower (results shown in table 4.5) than expected which is thought to be due to the large carbide grain size developed during sintering. In the case of Ni bonded material the hardness is higher than the binderless material, which must also be due to the much smaller grain size of the bonded material.

After sintering, the Hf/Ti molar ratio was determined by quantitative EDS analysis of 5 random regions and found to be 52.8/47.2 (std deviation: 0.56) in the Ni bonded material and 52.5/47.5 (standard deviation: 0.42) in the binderless materials where sintering occurred at a higher temperature. The decrease in standard deviation confirms progress towards a more homogeneous material.



## 4.5 Characterization of sintered HfC+ TiC with 4wt% Ni produced from mixed (and not milled) powders

This material was again produced by hot pressing at 1650°C and 30 MPa

### 4.5.1 XRD results of sintered HfC + TiC with Ni at 1650°C

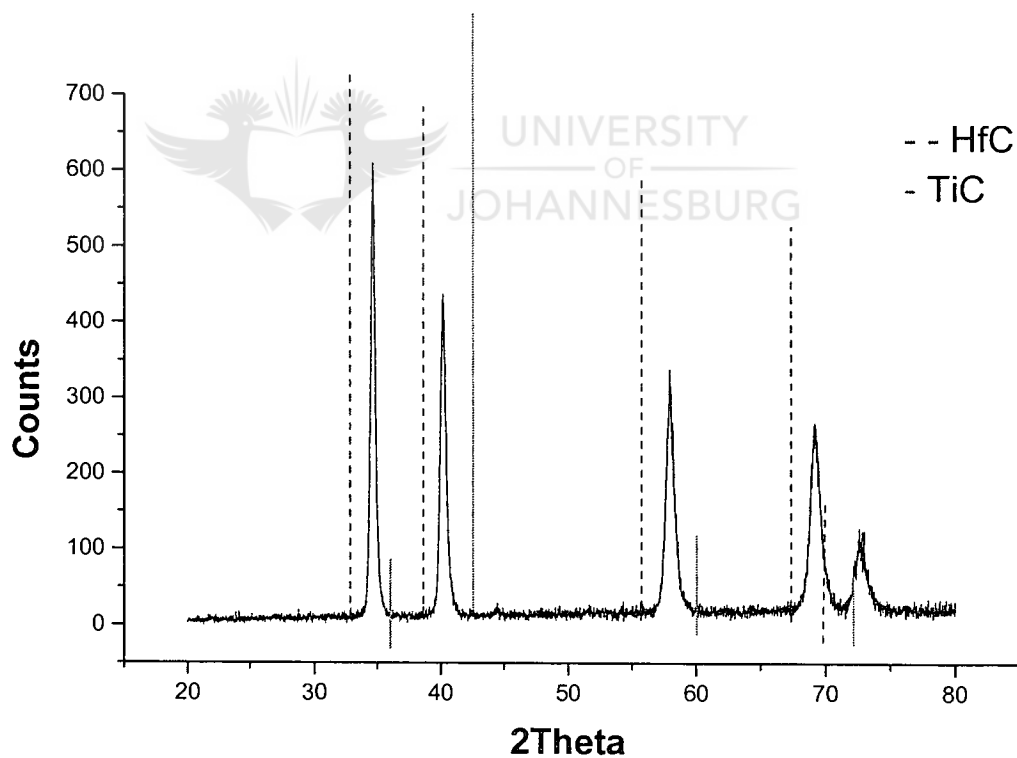
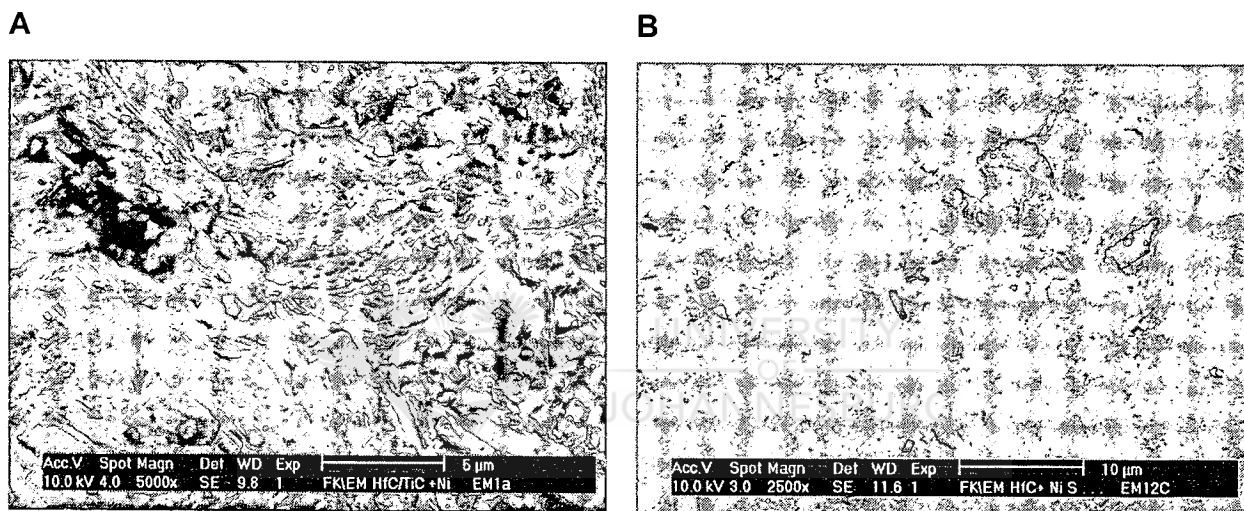


**Figure 4.24:** XRD results from mixed (not milled) HfC+TiC+ 4wt% Ni hot pressed at 1650°C and 30 MPa. The d-values are in Appendix 3

4.5.2 SEM micrographs of mixed (not milled) HfC+TiC+ 4wt%  
sintered at 1650°C



**A**= HfC+TiC+ 4% Ni fracture surface

**B**= HfC+TiC+ 4% Ni polished surface

**Figure 4.25:** SEM micrographs of mixed (not milled) HfC+TiC+ 4wt% Ni hot  
pressed at 1650°C 30 MPa.

**4.5.3 EDS results from mixed (not milled) HfC+TiC+ 4wt% Ni sintered at 1650°C**

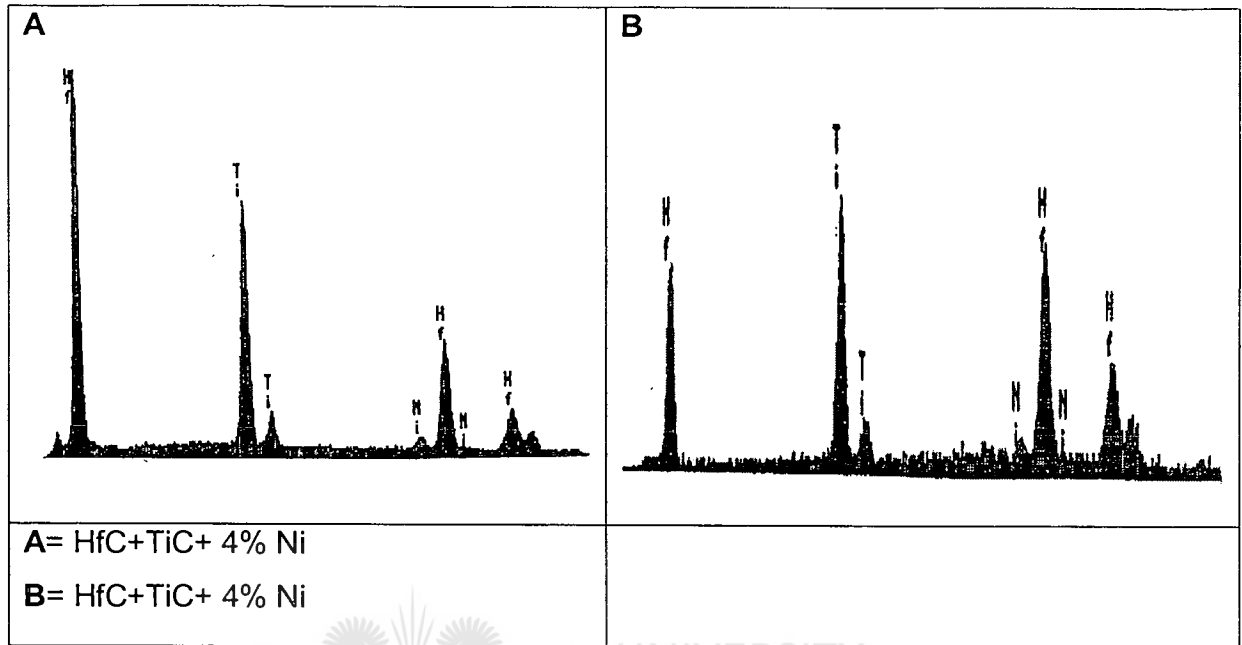


**Figure 4.26:** EDS spectra of mixed (not milled) HfC+TiC+ 4wt% Ni hot pressed at 1650°C and 30 mPa. A is from lighter regions and B from dark regions

**4.5.4 Hardness Results**

**Table 4.6:** Vickers Hardness for sintered HfC+TiC+4wt% Ni from mixed (not milled) powders

Load	HfC +TiC + 4% Ni Sintered at 1650°C
1kg	2359 Hv
5kg	2124 Hv
10kg	2185 Hv
30kg	2114 Hv

#### 4.5.5 Discussion

74wt%HfC, 22 wt% TiC and 4wt % Ni were mixed using the micronizing mill for 3 hours and hot pressed at 1650°C and 30 MPa. The sintering occurred with the formation of a liquid phase. The XRD results of in figure 4.24 show that a solid solution of (Hf, Ti) C was formed during sintering. On account of the mutual solid solubility of the two carbides vacancy interdiffusion controlled the solution as well as the sintering process, assisted by the high concentration of vacancies in the starting powders. Since the interdiffusion of HfC into TiC did not occur at the same rate as the diffusion of TiC into HfC (as expected, on account of different melting points of the two materials) diffusion porosity was observed in some of (Hf,Ti)C grains shown on the fracture surface in figure 4.25A.

EDS analysis was done on the sintered material, and inhomogeneity of the material was observed. Figure 4.26A shows clearly that the lighter areas are rich in Hf and and 4.26B that dark areas one rich in Ti. The hardness of the material was lower compared to pre-alloyed (Hf,Ti)C 4 wt% Ni. Grain size could not be observed clearly because an etchant has not being found yet.

## 4.6 Characterization of materials produced from high-energy dry milled HfC + TiC+C with and without Ni

### 4.6.1 XRD results from sintered high-energy milled HfC + TiC+ C powder without Ni at 2000°C

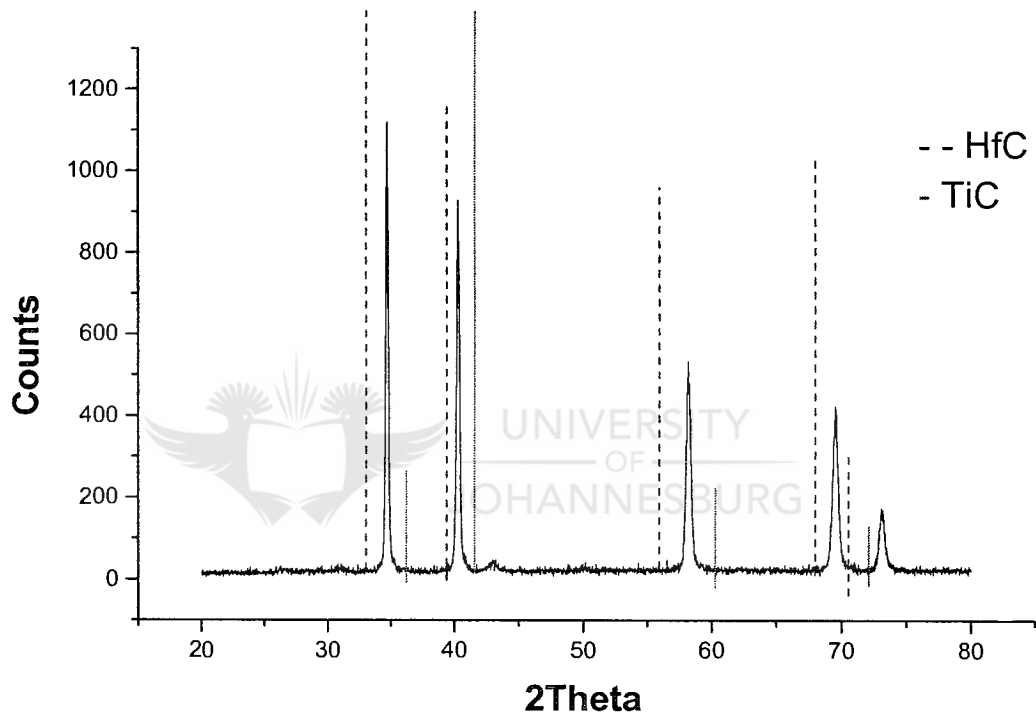


**Figure 4.27:** XRD results from high-energy milled HfC + TiC+ C powder sintered without Ni at 2000°C. The d-values are in Appendix 3.



4.6.2 XRD results from sintered high-energy milled HfC + TiC + C  
powders with 4wt% Ni at 1650°C

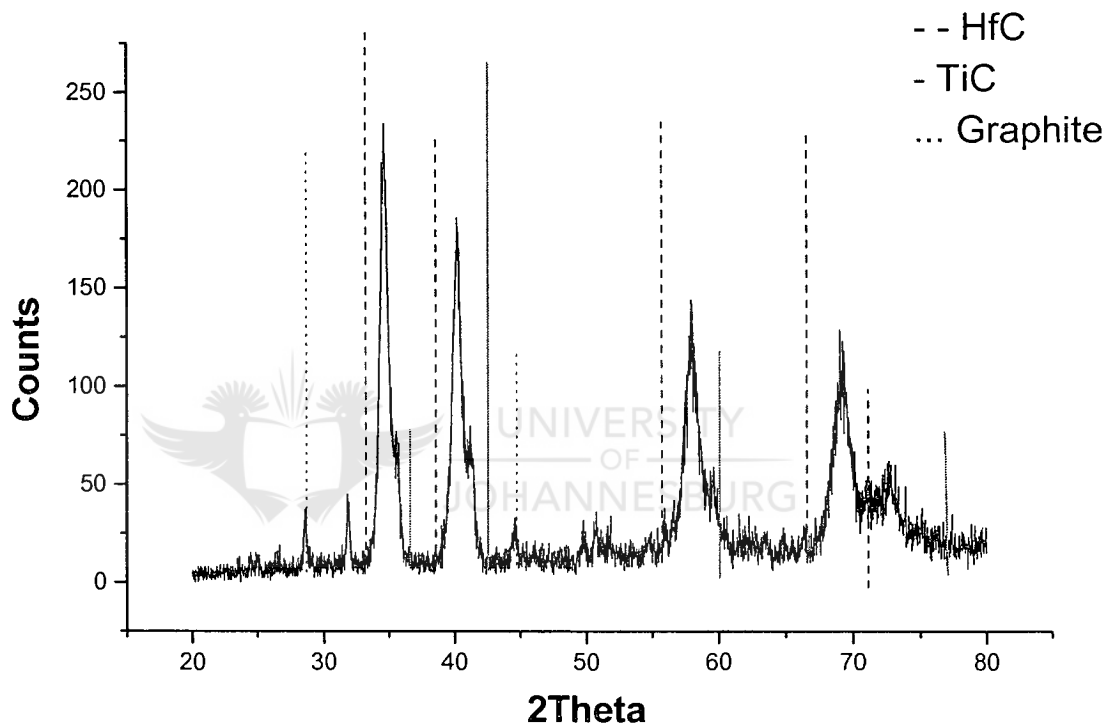
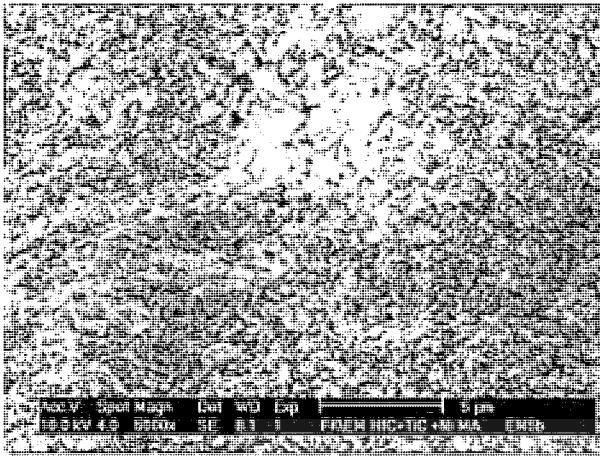


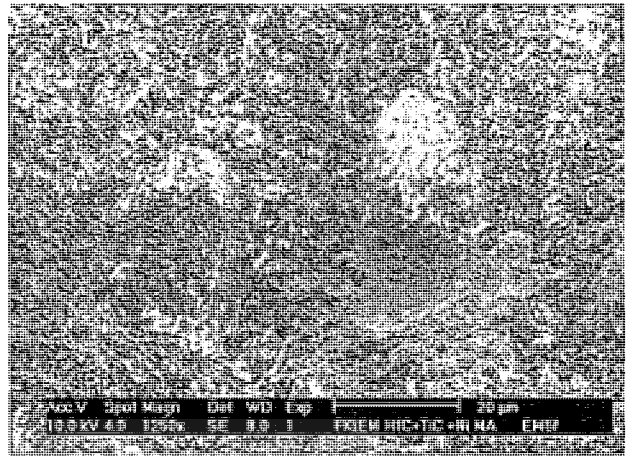
Figure 4.28: XRD results from high-energy milled HfC + TiC + C powder sintered with 4wt% Ni at 1650°C. The d-values are in Appendix 3.

4.6.3 SEM Micrographs of sintered High- energy dry milled  
HFC+TiC+ C powder with and without Ni. Fracture surfaces

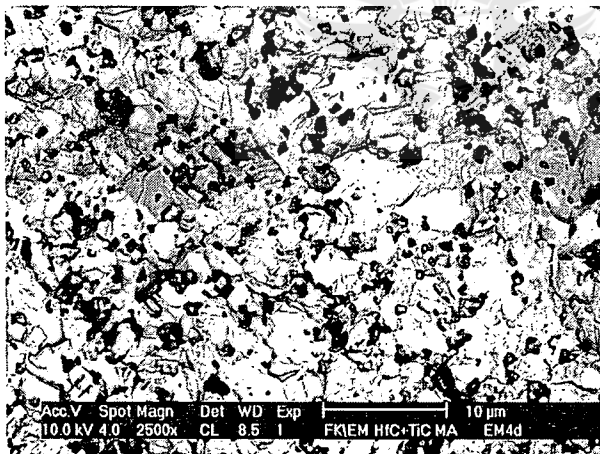
A



B



C



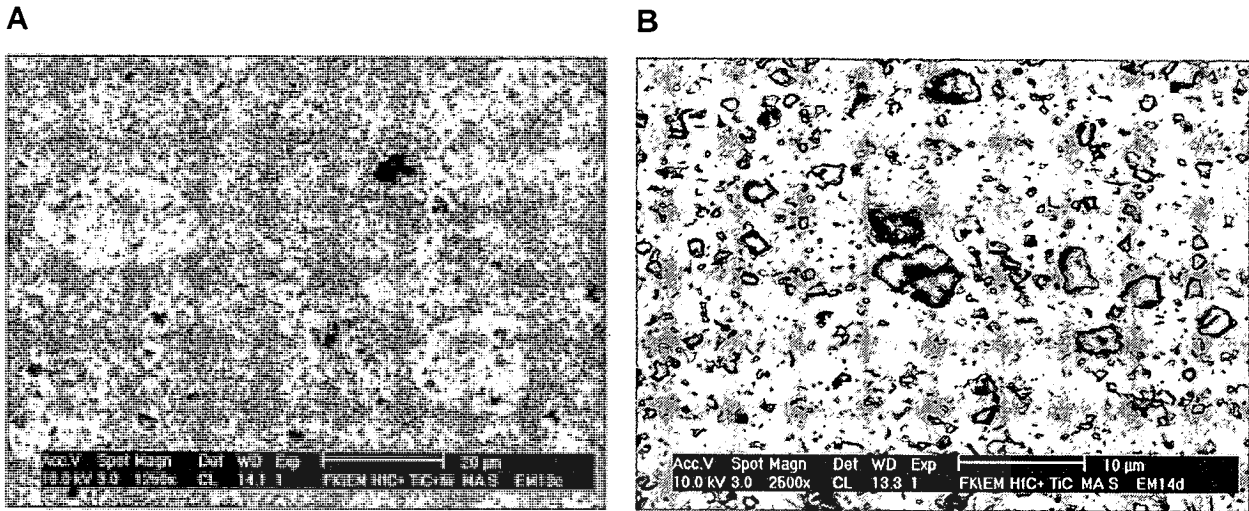
A= HFC+TiC+ C +4% Ni sintered at 1650°C

B= HFC+TiC+C +4% Ni sintered at 1650°C

C= HFC+TiC+C sintered at 2000°C

Figure 4.29: SEM fractographs of sintered high- energy dry milled HFC+TiC+C with and without Ni.

4.6.4 SEM Micrographs of sintered high- energy dry milled  
HfC+TiC+C with and without Ni. Polished surfaces



A= HfC+TiC+ C +4% Ni sintered at  
1650°C

B= HfC+TiC+ C sintered at 2000°C

Figure 4.30: SEM Micrographs of polished surface of High- energy dry milled  
HfC+TiC with and without Ni.

4.6.5 Examples of EDS results from High- energy dry milled  
HFC+TiC+ C with and without 4wt% Ni. Lighter and darker regions

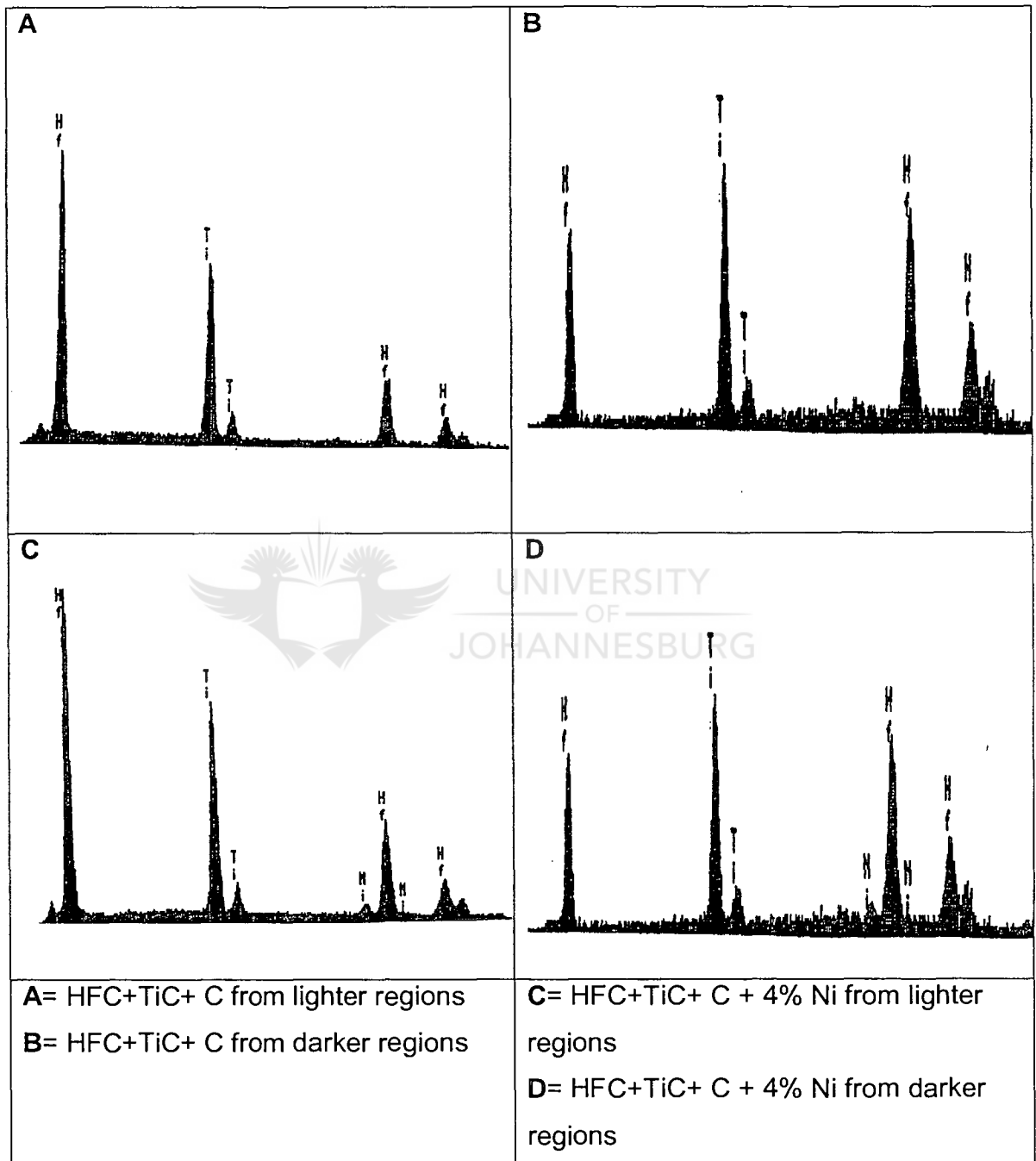


Figure 4.31: EDS spectra of High- energy dry milled HFC+TiC+ C with and without 4% Ni.

**4.6.6 Results of Vickers Hardness of sintered High- energy dry milled HfC+TiC+ C with and without Ni**

**Table 4.7:** Vickers Hardness for High- energy dry milled HfC+TiC

Load	HfC +TiC + carbon black MA Sintered at 2000°C	HfC +TiC + carbon black +4% Ni MA <sup>1</sup> and MM <sup>2</sup> Sintered at 1650°C
1kg	1806.6 Hv	634 Hv
5kg	1736 Hv	522 Hv
10kg	1557 Hv	577 Hv
30kg	1415 Hv	548.8 Hv

MA<sup>1</sup> = milled under mechanical alloying conditions to mix the carbides

MM<sup>2</sup>= milled in a micronizing mill to mix Ni and carbides

**4.6.7 Density resultsof sintered High- energy dry milled HfC+TiC+C with and without Ni**

**Table 4.8:** Density measurements of High-energy dry milled HfC+TiC

Material	Density
Theoretical density (Hf,Ti)C	9.36 g/cm <sup>3</sup>
HfC+TiC+ C	7.8 g/cm <sup>3</sup>
HfC+TiC+ C + Ni	7.23 g/cm <sup>3</sup>

#### 4.6.8 Discussion

76 wt % HfC, 22 wt%TiC and 2wt% carbon black was the composition of the high-energy milled HfC+TiC+ C powders. Carbon black was added in order to compensate for carbon loss during milling and for substoichiometry of the HfC and TiC powders.

After sintering HfC+TiC+ C at 2000°C a solid solution was formed as shown in figure 4.27 by the XRD results. 4 wt % Ni was added to the material and micronized milled for 4 hours. Then the powder was sintered at 1650°C and the results showed that a solid solution was formed after sintering as observed in figure 4.28. The XRD results in figure 4.28 indicated that the solid solution (Hf,Ti) C had formed but the peaks width was very broad, while after sintering at 2000°C the XRD peaks had narrowed significantly with sintering occurring through interdiffusion of Hf and Ti atoms from and into (Hf, Ti)C particles of unequal composition at different diffusion rates.

Both the density and hardness (table 4.7 and 4.8) are very low because of the porosity and inhomogeneous structure. Figure 4.29A shows that the binderless material had a much finer grain size than the material in figure 4.29B. Grain growth occurred during sintering but from starting powders of crystalline size of the order of nm's. Most of the pores contained Ti- rich particles.

Figure 4.29C shows the inhomogeneous microstructure of the material without binder produced from the high –energy milled powder. Agglomerates formed during milling with Ni remained intact as shown in figure 4.29B, and created islands of Hf- rich regions within Ti- rich regions. The agglomerates proved to be poorly bonded to the rest of the structure since fracture was found to propagate preferably along their boundaries.

## 5. Final Discussion and Conclusion

This investigation has showed that sintered (Hf, Ti) C material can be produced either starting from pre-reacted (Hf, Ti) C powder or from single TiC and HfC powders because during sintering the single carbides form a (Hf, Ti) C solid solution by interdiffusion. However, the problem seems to be that interdiffusion takes place at different diffusion rates, which leads to incomplete homogenization and porosity (as seen in figures 4.25 and 4.30). Better homogenization and lower porosity is obtained when starting from pre-reacted powders (see figure 4.22).

The hardness values obtained from the samples produced during this investigation are much lower than the maximum value (4600 Hv) that can be reached by this material. The low values obtained from the samples produced from individual TiC and HfC powders are thought to be due to the high porosity levels and inhomogeneity. The low values obtained from a pre-reacted powder are thought to be due to large grain size ( $>5-10\ \mu\text{m}$ ).

High-energy dry milled powders gave inferior (lower) results to simply mixed HfC and TiC powders. This is thought to be due to the strong agglomerates  $\gg 10\ \mu\text{m}$  formed during dry high-energy milling (see figure 4.29B).

Despite the limitations of the results obtained, the idea is that (Hf, Ti) C has potential as a hard material because it is easily sintered to high density and has a respectable hardness ( $\gg 2000\ \text{Hv}$ ) even at grain sizes larger than  $5-10\ \mu\text{m}$ . Therefore it seems to be worth continuing to search for the best processing route for this material.

## 6. References

Adams, R.P. Copeland, B.K. 1968. **Bureau of Mine**. Report 7137. June 1968.

Brizes, W.F. 1970. **SRCC**. Report 117.

Cahn, R. Haasen, W. 1996. **Physical Metallurgy**. 1. Elsevier Science B. V. Netherlands: 16,18,19,24.

Edmund, K. 1967. **The Refractory Carbides**.2. New York. Academic Press: 35.

Jangg, G. Kieffer, R. Usner. 1968. **HfC System**. Journal Less Common Metal. 14:169.

Kieffer, R. Ettmayer, P and Freudhofmeier, M. 1971. **Mod Dev Powder Metallurgy**: 201.

Mun, S. Kang, S.1999. **Effect of HfC addition on the microstructure of Ti(CN)-Ni cermet system**. Materials Science and Engineering. Seoul National University, Korea: 3,4.

Murray, J.L. 1987. **Binary Alloy phase diagrams**.1.2.3. USA. William W. Scotts Jr: 890.

Okamoto, H. 1990. **Binary phase diagram**.1.2.3. USA. William W. Scotts Jr: 851.

Panderno , U.N. 1967.**HfC**. Inorg. Materials. 3. AN USSR: 1170-1184.



Perry, A.J. 1987. **The Refractories HfC and HfN**. Powder Metallurgy. International. 19. Verlag Schmid :17,29, 31-36.

Ramqvist, L. 1969. **Preparation, properties and electronic structure of refractory carbides and related compounds**, Jernkont. Ann. **153**. Almqvist & Wiksells: 1-21.

Ramqvist, L. 1987. **Refractory Carbides**. Powder Metallurgy International.1:2-21.

Sara, R.V. 1965. **HfC System**. Trans AIME. 233: 1683.

Upadhyaya G.S. 1996. **"Nature and Properties of Refractory Carbides"**. Nova Science Publ, New York, USA: 124,125,126,422, 456, 459 and 458.

West, J. 1962. **High Temperature Studies**. Foreign Moscow literature Press: 185.

Xinkunk, Z. Kunyu, Z. Baochang, C. Qiushi, L. Xiuqin, Z. Tieli, C. Yunsheng. S. 2001. **Synthesis of nanocrystalline TiC powders by mechanical alloying**. Materials Science & Eng. Elsevier Science B.V, China:103-105.

## Appendix 1

### d-values of HfC

Theoretical d-values of HfC	d-values of HfC as received
2.68	2.66
2.32	2.30
1.64	1.63

### d-values of TiC

Theoretical d-values of TiC	d-values of TiC as received
2.50	2.48
2.16	2.15
1.53	1.52

## Appendix 2

d-values of  $(\text{Hf}_{0.5}\text{Ti}_{0.5})\text{C}_{0.8}$

d-values of $(\text{Hf}_{0.5}\text{Ti}_{0.5})\text{C}_{0.8}$ powder as received	d-values of $(\text{Hf}_{0.5}\text{Ti}_{0.5})\text{C}_{0.8}$ After sintered at 2000°C	d-values of $(\text{Hf}_{0.5}\text{Ti}_{0.5})\text{C}_{0.8}$ After sintered at 1650°C
2.60	2.58	2.59
2.24	2.37	2.24
1.58	1.58	1.58



UNIVERSITY  
OF  
JOHANNESBURG

### Appendix 3

d-values of HfC+TiC+Ni and HfC+TiC+C high-energy milled

<b>d-values of mixed HfC+TiC After sintered at 1650°C</b>	<b>d-values of HfC+TiC+C high-energy milled After sintered at 2000°C</b>	<b>d-values of HfC+TiC+C +Ni high-energy milled After sintered at 1650°C</b>
2.59	2.58	2.59
2.23	2.23	2.24
1.58	1.58	1.59

# Appendix 4

## HfC particle size analysis as received powder

Version 1.2b

Thu, 02 May, 2002 2:58PM

HfC - Lot 67802 :Run Number 4

Saved as ETM\_01

Source: Analysed

Measured on: Thu, 02 May, 2002 2:58PM

Presentation: 25SD

Very Polydisperse model

Volume Result

Focus = 45 mm.

Residual = 1.650 %

Concentration = 0.005 %

Obscuration = 17.37 %

d (0.5) = 2.15 µm

d (0.1) = 1.05 µm

d (0.9) = 4.40 µm

D [4, 3] = 2.50 µm

Span = 1.56

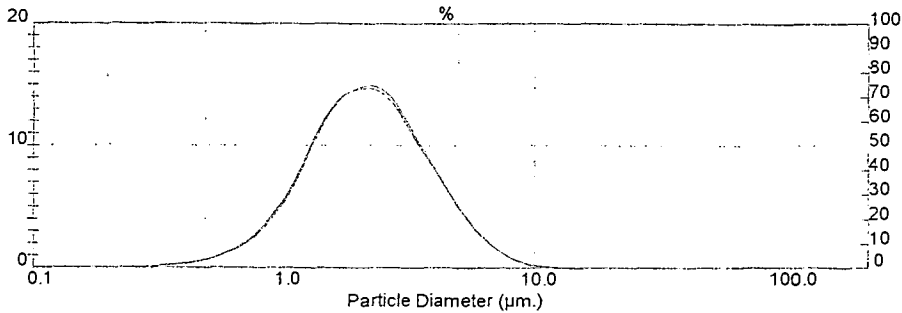
Sauter Mean (D[3,2]) = 1.80 µm

Mode = 2.21 µm

Specific Surface Area = 3.3410 sq. m. / gm

Density = 1.00 gm. / c.c.

Size (Lo) µm	Result In %	Size (Hi) µm	Result Below %	Size (Lo) µm	Result In %	Size (Hi) µm	Result Below %
0.05	0.01	0.12	0.01	2.83	11.71	3.49	80.58
0.12	0.01	0.15	0.01	3.49	8.63	4.30	89.21
0.15	0.02	0.19	0.03	4.30	5.60	5.29	94.81
0.19	0.04	0.23	0.08	5.29	3.08	6.52	97.89
0.23	0.08	0.28	0.16	6.52	1.42	8.04	99.31
0.28	0.17	0.35	0.32	8.04	0.50	9.91	99.81
0.35	0.32	0.43	0.64	9.91	0.15	12.21	99.97
0.43	0.62	0.53	1.26	12.21	0.03	15.04	100.00
0.53	1.17	0.65	2.43	15.04	0.00	18.54	100.00
0.65	2.19	0.81	4.62	18.54	0.00	22.84	100.00
0.81	3.97	1.00	8.59	22.84	0.00	28.15	100.00
1.00	6.91	1.23	15.50	28.15	0.00	34.69	100.00
1.23	10.52	1.51	26.02	34.69	0.00	42.75	100.00
1.51	13.72	1.86	39.74	42.75	0.00	52.68	100.00
1.86	14.99	2.30	54.73	52.68	0.00	64.92	100.00
2.30	14.15	2.83	68.88	64.92	0.00	80.00	100.00



Malvern Instruments Ltd.  
Malvern, U.K.

MasterSizer X Ver. 1.2b  
Serial No. 6559

02 May 02 14:58

## Appendix 5

### HfC particle size analysis after 2hrs high-energy dry milling

Version 1.2b

Thu, 02 May, 2002 3:05PM

HfC - Milled 2hr :Run Number 3

Saved as ETM\_01

Sample File Name: ETM\_01 , Record: 8

Source: Analysed

Measured on: Thu, 02 May, 2002 3:02PM Last saved on: Thu, 02 May, 2002 3:02PM

Presentation: 2S\$D

Very Polydisperse model

Volume Result

Focus = 45 mm.

Residual = 1.472 %

Concentration = 0.004 %

Obscuration = 18.00 %

d (0.5) = 4.86  $\mu$ m

d (0.1) = 0.64  $\mu$ m

d (0.9) = 17.27  $\mu$ m

D [4, 3] = 7.24  $\mu$ m

Span = 3.42

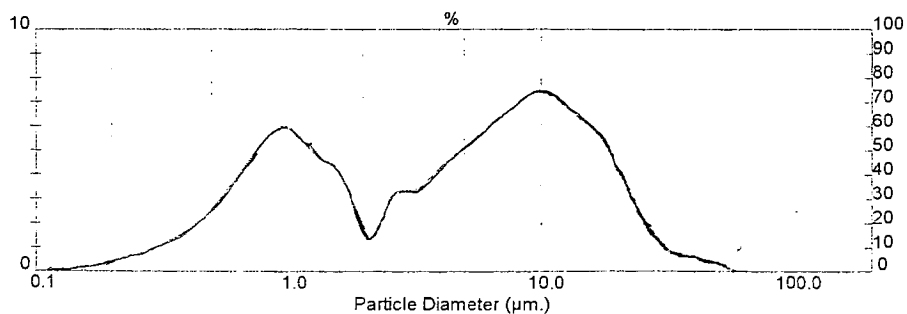
Sauter Mean (D[3,2]) = 1.61  $\mu$ m

Mode = 10.10  $\mu$ m

Specific Surface Area = 3.7270 sq. m. / gm

Density = 1.00 gm. / c.c.

Size (Lo) $\mu$ m	Result In %	Size (Hi) $\mu$ m	Result Below %	Size (Lo) $\mu$ m	Result In %	Size (Hi) $\mu$ m	Result Below %
0.05	0.21	0.12	0.21	2.83	3.41	3.49	42.96
0.12	0.11	0.15	0.31	3.49	4.18	4.30	47.14
0.15	0.21	0.19	0.52	4.30	4.99	5.29	52.13
0.19	0.44	0.23	0.96	5.29	5.81	6.52	57.94
0.23	0.75	0.28	1.71	6.52	6.61	8.04	64.55
0.28	1.15	0.35	2.86	8.04	7.41	9.91	71.96
0.35	1.67	0.43	4.52	9.91	7.45	12.21	79.40
0.43	2.41	0.53	6.93	12.21	6.61	15.04	86.02
0.53	3.48	0.65	10.42	15.04	5.80	18.54	91.81
0.65	4.84	0.81	15.25	18.54	3.93	22.84	95.74
0.81	5.86	1.00	21.11	22.84	2.18	28.15	97.92
1.00	5.75	1.23	26.86	28.15	0.95	34.69	98.86
1.23	4.54	1.51	31.41	34.69	0.65	42.75	99.51
1.51	3.76	1.86	35.17	42.75	0.42	52.68	99.93
1.86	1.37	2.30	36.54	52.68	0.07	64.92	100.00
2.30	3.01	2.83	39.55	64.92	0.00	80.00	100.00



Malvern Instruments Ltd.  
Malvern, U.K.

MasterSizer X Ver. 1.2b  
Serial No. 6559

02 May 02 15:05

## Appendix 6

### HfC particle size analysis after 6hrs high-energy dry milling

Version 1.2b

Thu, 02 May, 2002 3:10PM

HfC - Milled 6hr :Run Number 1

Saved as ETM\_01

Sample File Name: ETM\_01 , Record: 9

Source: Analysed

Measured on: Thu, 02 May, 2002 3:08PM Last saved on: Thu, 02 May, 2002 3:08PM

Presentation: 2\$\$D

Very Polydisperse model

Volume Result

Focus = 45 mm.

Residual = 1.542 %

Concentration = 0.003 %

Obscuration = 12.19 %

d (0.5) = 3.37 µm

d (0.1) = 0.72 µm

d (0.9) = 13.99 µm

D [4, 3] = 5.67 µm

Span = 3.94

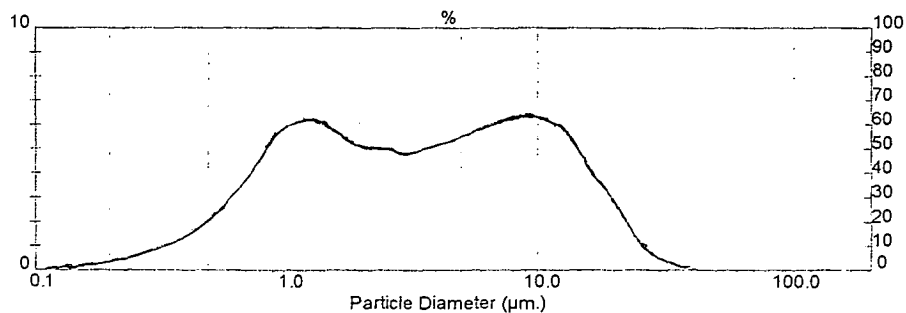
Sauter Mean (D[3,2]) = 1.67 µm

Mode = 8.76 µm

Specific Surface Area = 3.6032 sq. m. / gm

Density = 1.00 gm. / c.c.

Size (Lo) µm	Result In %	Size (Hi) µm	Result Below %	Size (Lo) µm	Result In %	Size (Hi) µm	Result Below %
0.05	0.07	0.12	0.07	2.83	4.91	3.49	50.85
0.12	0.12	0.15	0.20	3.49	5.15	4.30	56.00
0.15	0.21	0.19	0.41	4.30	5.45	5.29	61.45
0.19	0.39	0.23	0.80	5.29	5.91	6.52	67.36
0.23	0.62	0.28	1.41	6.52	6.30	8.04	73.66
0.28	0.93	0.35	2.34	8.04	6.45	9.91	80.11
0.35	1.34	0.43	3.68	9.91	6.18	12.21	86.29
0.43	1.94	0.53	5.63	12.21	5.47	15.04	91.76
0.53	2.82	0.65	8.44	15.04	3.94	18.54	95.70
0.65	4.03	0.81	12.48	18.54	2.64	22.84	98.35
0.81	5.36	1.00	17.84	22.84	1.12	28.15	99.46
1.00	6.24	1.23	24.08	28.15	0.43	34.69	99.89
1.23	6.08	1.51	30.17	34.69	0.08	42.75	99.97
1.51	5.63	1.86	35.79	42.75	0.02	52.68	99.99
1.86	5.18	2.30	40.98	52.68	0.00	64.92	100.00
2.30	4.96	2.83	45.94	64.92	0.00	80.00	100.00



Malvern Instruments Ltd.  
Malvern, U.K.

MasterSizer X Ver. 1.2b  
Serial No. 6559

02 May 02 15:10

# Appendix 7

## TiC particle size analysis as received powder

Version 1.2b

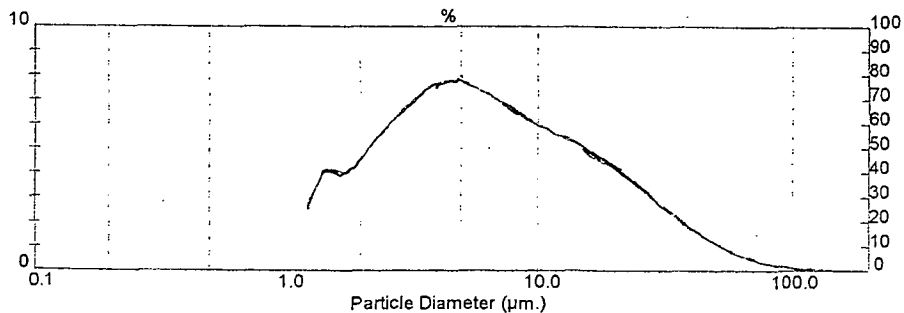
Mon, 26 Mar, 2001 9:14AM

Titanium Carbide :Run Number 4

Saved as ETM\_01  
 Sample File Name: ETM\_01 , Record: 2 Source: Analysed  
 Measured on: Mon, 26 Mar, 2001 9:13AM Last saved on: Mon, 26 Mar, 2001 9:13AM

Presentation: 2\$\$D  
 Very Polydisperse model Volume Result Focus = 300 mm.  
 Residual = 0.183 % Concentration = 0.011 % Obscuration = 19.22 %  
 d (0.5) = 5.77 µm d (0.1) = 1.70 µm d (0.9) = 24.04 µm  
 D [4, 3] = 10.29 µm Span = 3.87 Mode = 4.62 µm  
 Sauter Mean ( D[3,2] ) = 3.81 µm Density = 1.00 gm. / c.c.  
 Specific Surface Area = 1,5766 sq. m. / gm

Size (Lo) µm	Result In %	Size (Hi) µm	Result Below %	Size (Lo) µm	Result In %	Size (Hi) µm	Result Below %
0.50	4.84	1.32	4.84	25.46	2.91	31.01	93.88
1.32	3.93	1.60	8.77	31.01	2.18	37.79	96.06
1.60	4.02	1.95	12.79	37.79	1.54	46.03	97.60
1.95	5.03	2.38	17.83	46.03	1.03	56.09	98.63
2.38	6.08	2.90	23.91	56.09	0.63	68.33	99.26
2.90	6.96	3.53	30.87	68.33	0.37	83.26	99.63
3.53	7.60	4.30	38.47	83.26	0.20	101.44	99.83
4.30	7.80	5.24	46.27	101.44	0.10	123.59	99.93
5.24	7.50	6.39	53.77	123.59	0.04	150.57	99.98
6.39	6.85	7.78	60.61	150.57	0.02	183.44	99.99
7.78	6.28	9.48	66.89	183.44	0.00	223.51	100.00
9.48	5.81	11.55	72.70	223.51	0.00	272.31	100.00
11.55	5.42	14.08	78.12	272.31	0.00	331.77	100.00
14.08	4.93	17.15	83.05	331.77	0.00	404.21	100.00
17.15	4.31	20.90	87.36	404.21	0.00	492.47	100.00
20.90	3.62	25.46	90.98	492.47	0.00	600.00	100.00



Malvern Instruments Ltd.  
 Malvern, U.K.

MasterSizer X Ver. 1.2b  
 Serial No. 6559

26 Mar 01 09:14



## Appendix 8

### TiC particle size analysis after 2hrs high-energy dry milling

Version 1.2b

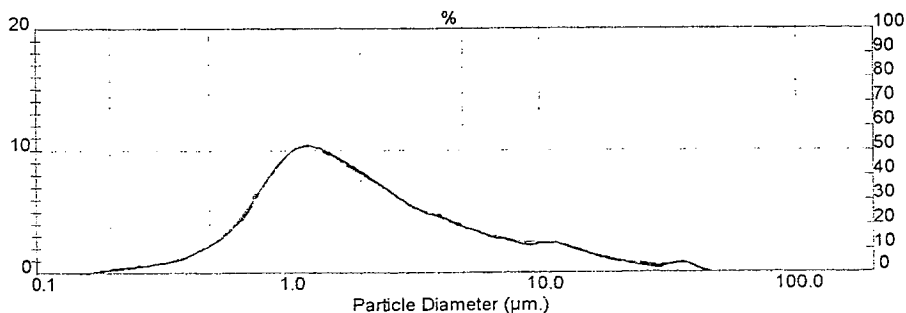
Thu, 02 May, 2002 3:16PM

TiC - Milled 2hr :Run Number 3

Saved as ETM\_01  
 Sample File Name: ETM\_01 , Record: 13 Source: Input  
 Measured on: Last saved on: Thu, 02 May, 2002 3:16PM

Presentation: 2\$SD  
 Polydisperse model Volume Result Focus = 0 mm.  
 Residual = 0.000 % Concentration = 0.000 % Obscuration = 0.00 %  
 d (0.5) = 1.75 µm d (0.1) = 0.69 µm d (0.9) = 9.29 µm  
 D [4, 3] = 3.79 µm Span = 4.92 Mode = 1.24 µm  
 Sauter Mean ( D[3,2] ) = 1.37 µm Density = 1.00 gm. / c.c.  
 Specific Surface Area = 4.3767 sq. m. / gm

Size (Lo) µm	Result In %	Size (Hi) µm	Result Below %	Size (Lo) µm	Result In %	Size (Hi) µm	Result Below %
0.05	0.02	0.12	0.02	2.83	5.61	3.49	73.04
0.12	0.05	0.15	0.07	3.49	4.87	4.30	77.91
0.15	0.13	0.19	0.20	4.30	4.03	5.29	81.94
0.19	0.28	0.23	0.48	5.29	3.33	6.52	85.27
0.23	0.49	0.28	0.97	6.52	2.96	8.04	88.23
0.28	0.82	0.35	1.79	8.04	2.55	9.91	90.79
0.35	1.32	0.43	3.11	9.91	2.53	12.21	93.31
0.43	2.15	0.53	5.26	12.21	1.94	15.04	95.25
0.53	3.55	0.65	8.81	15.04	1.52	18.54	96.77
0.65	5.75	0.81	14.56	18.54	1.07	22.84	97.84
0.81	8.42	1.00	22.97	22.84	0.75	28.15	98.59
1.00	10.35	1.23	33.32	28.15	0.71	34.69	99.30
1.23	10.11	1.51	43.44	34.69	0.69	42.75	99.99
1.51	9.16	1.86	52.59	42.75	0.01	52.68	100.00
1.86	8.03	2.30	60.62	52.68	0.00	64.92	100.00
2.30	6.80	2.83	67.42	64.92	0.00	80.00	100.00



Malvern Instruments Ltd.  
 Malvern, U.K.

MasterSizer X Ver. 1.2b  
 Serial No. 6559

02 May 02 15:16

## Appendix 9

### TiC particle size analysis after 6hrs high-energy dry milling

Version 1.2b

Thu, 02 May, 2002 3:23PM

TiC - Milled 6hr :Run Number 2

Saved as ETM\_01

Sample File Name: ETM\_01 , Record: 13

Source: Input

Measured on:

Last saved on: Thu, 02 May, 2002 3:22PM

Presentation: 2\$\$D

Polydisperse model

Volume Result

Focus = 0 mm.

Residual = 0.000 %

Concentration = 0.000 %

Obscuration = 0.00 %

d (0.5) = 4.55  $\mu$ m

d (0.1) = 0.76  $\mu$ m

d (0.9) = 33.96  $\mu$ m

D [4, 3] = 12.11  $\mu$ m

Span = 7.30

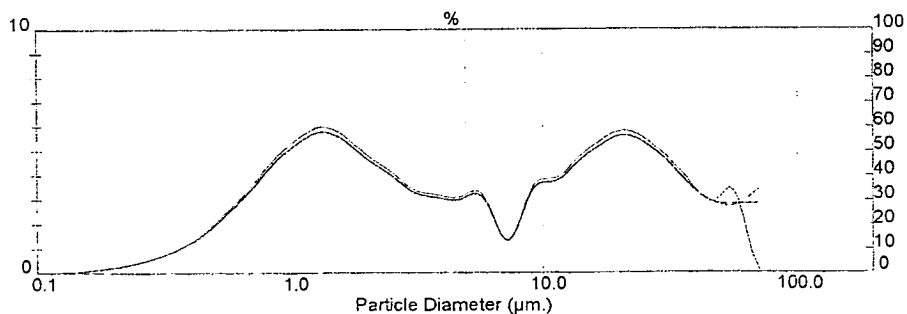
Mode = 1.38  $\mu$ m

Sauter Mean ( D[3,2] ) = 1.92  $\mu$ m

Specific Surface Area = 3.1247 sq. m. / gm

Density = 1.00 gm. / c.c.

Size (Lo) $\mu$ m	Result In %	Size (Hi) $\mu$ m	Result Below %	Size (Lo) $\mu$ m	Result In %	Size (Hi) $\mu$ m	Result Below %
0.05	0.07	0.12	0.07	2.83	3.49	3.49	45.91
0.12	0.05	0.15	0.12	3.49	3.26	4.30	49.16
0.15	0.14	0.19	0.26	4.30	3.15	5.29	52.32
0.19	0.27	0.23	0.53	5.29	3.18	6.52	55.50
0.23	0.47	0.28	1.00	6.52	1.40	8.04	56.90
0.28	0.77	0.35	1.78	8.04	3.45	9.91	60.35
0.35	1.20	0.43	2.97	9.91	3.90	12.21	64.25
0.43	1.82	0.53	4.79	12.21	4.70	15.04	68.95
0.53	2.67	0.65	7.46	15.04	5.46	18.54	74.41
0.65	3.71	0.81	11.17	18.54	5.87	22.84	80.28
0.81	4.79	1.00	15.96	22.84	5.50	28.15	85.77
1.00	5.70	1.23	21.66	28.15	4.66	34.69	90.43
1.23	5.94	1.51	27.60	34.69	3.62	42.75	94.05
1.51	5.67	1.86	33.27	42.75	3.01	52.68	97.06
1.86	4.96	2.30	38.23	52.68	2.91	64.92	99.97
2.30	4.19	2.83	42.42	64.92	0.03	80.00	100.00



Malvern Instruments Ltd.  
Malvern, U.K.

MasterSizer X Ver. 1.2b  
Serial No. 6559

02 May 02 15:23

# Appendix 10

## (Hf<sub>0.5</sub>Ti<sub>0.5</sub>)C<sub>0.8</sub> particle size analysis as received powder

Version 1.2b

Wed, 18 Jul, 2001 10:31AM

HFTIC :Run Number 1

Saved as ETM\_01

Sample File Name: ETM\_01 , Record: 3

Source: Analysed

Measured on: Wed, 18 Jul, 2001 10:31AM Last saved on: Wed, 18 Jul, 2001 10:31AM

Presentation: 2\$SD

Very Polydisperse model

Volume Result

Focus = 300 mm.

Residual = 0.364 %

Concentration = 0.007 %

Obscuration = 23.36 %

d (0.5) = 2.14 µm

d (0.1) = 1.01 µm

d (0.9) = 5.56 µm

D [4, 3] = 3.03 µm

Span = 2.13

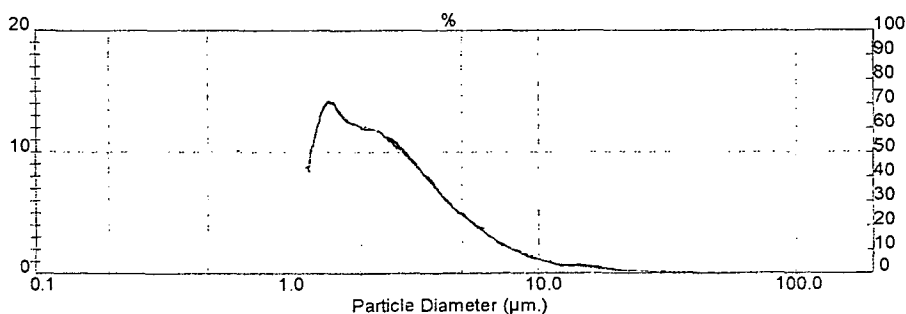
Sauter Mean (D[3,2]) = 1.79 µm

Mode = 1.51 µm

Specific Surface Area = 3.3442 sq. m. / gm

Density = 1.00 gm. / c.c.

Size (Lo) µm	Result In %	Size (Hi) µm	Result Below %	Size (Lo) µm	Result In %	Size (Hi) µm	Result Below %
0.50	18.12	1.32	18.12	25.46	0.18	31.01	99.73
1.32	13.43	1.60	31.55	31.01	0.12	37.79	99.85
1.60	12.77	1.95	44.32	37.79	0.08	46.03	99.93
1.95	12.13	2.38	56.45	46.03	0.04	56.09	99.97
2.38	10.93	2.90	67.38	56.09	0.02	68.33	99.99
2.90	9.07	3.53	76.45	68.33	0.01	83.26	100.00
3.53	7.04	4.30	83.49	83.26	0.00	101.44	100.00
4.30	5.22	5.24	88.71	101.44	0.00	123.59	100.00
5.24	3.80	6.39	92.51	123.59	0.00	150.57	100.00
6.39	2.56	7.78	95.07	150.57	0.00	183.44	100.00
7.78	1.64	9.48	96.71	183.44	0.00	223.51	100.00
9.48	1.07	11.55	97.78	223.51	0.00	272.31	100.00
11.55	0.71	14.08	98.49	272.31	0.00	331.77	100.00
14.08	0.48	17.15	98.97	331.77	0.00	404.21	100.00
17.15	0.34	20.90	99.31	404.21	0.00	492.47	100.00
20.90	0.24	25.46	99.55	492.47	0.00	600.00	100.00



Malvern Instruments Ltd.  
Malvern, U.K.

MasterSizer X Ver. 1.2b  
Serial No. 6559

18 Jul 01 10:31

# Appendix 11

## HfC+TiC+ C powder particle size analysis after 12hrs high-energy dry milling

Version 1.2b

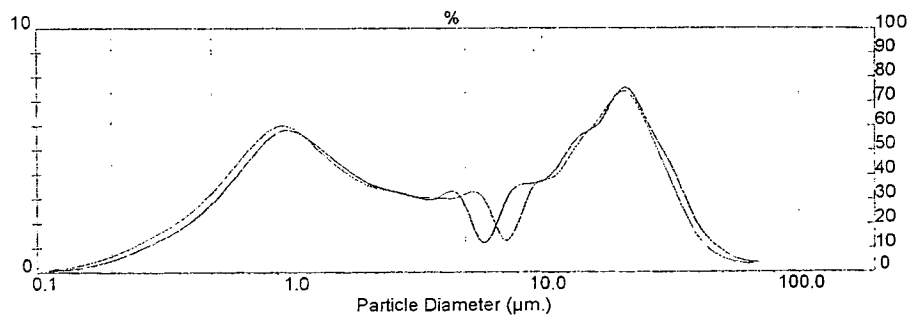
Thu, 02 May, 2002 3:25PM

TiC - HfC 12hr mill :Run Number 2

Saved as ETM\_01  
 Sample File Name: ETM\_01 , Record: 15 Source: Analysed  
 Measured on: Thu, 02 May, 2002 3:24PM Last saved on: Thu, 02 May, 2002 3:25PM

Presentation: 2\$SD  
 Very Polydisperse model Volume Result Focus = 45 mm.  
 Residual = 1.396 % Concentration = 0.006 % Obscuration = 26.66 %  
 d (0.5) = 4.08 µm d (0.1) = 0.59 µm d (0.9) = 26.57 µm  
 D [4, 3] = 10.13 µm Span = 6.37  
 Sauter Mean ( D[3,2] ) = 1.49 µm Mode = 20.64 µm  
 Specific Surface Area = 4.0301 sq. m. / gm Density = 1.00 gm. / c.c.

Size (Lo) µm	Result In %	Size (Hi) µm	Result Below %	Size (Lo) µm	Result In %	Size (Hi) µm	Result Below %
0.05	0.29	0.12	0.29	2.83	3.14	3.49	47.74
0.12	0.15	0.15	0.44	3.49	3.09	4.30	50.82
0.15	0.30	0.19	0.74	4.30	3.08	5.29	53.91
0.19	0.57	0.23	1.31	5.29	1.23	6.52	55.14
0.23	0.93	0.28	2.24	6.52	3.06	8.04	58.20
0.28	1.38	0.35	3.62	8.04	3.66	9.91	61.86
0.35	1.92	0.43	5.54	9.91	4.13	12.21	65.99
0.43	2.67	0.53	8.20	12.21	5.51	15.04	71.50
0.53	3.66	0.65	11.87	15.04	6.25	18.54	77.75
0.65	4.86	0.81	16.73	18.54	7.62	22.84	85.37
0.81	5.74	1.00	22.47	22.84	6.14	28.15	91.51
1.00	5.82	1.23	28.28	28.15	4.37	34.69	95.88
1.23	4.94	1.51	33.23	34.69	2.19	42.75	98.07
1.51	4.28	1.86	37.50	42.75	1.03	52.68	99.10
1.86	3.73	2.30	41.24	52.68	0.52	64.92	99.62
2.30	3.36	2.83	44.60	64.92	0.38	80.00	100.00



Malvern Instruments Ltd.  
 Malvern, U.K.

MasterSizer X Ver. 1.2b  
 Serial No. 6559

02 May 02 15:25